[AMERICAN JOURNAL OF SCIENCE, VOL. 293, APRIL, 1993, P. 257–296]

American Journal of Science

APRIL 1993

SCALING PROPERTIES OF TIME-SPACE KINETIC MASS TRANSPORT EQUATIONS AND THE LOCAL EQUILIBRIUM LIMIT

Peter C. Lichtner*

Hydrochemie Gruppe, Geologisches und
Mineralogisch-petrographisches Institut, Universität Bern,
Baltzer-Strasse 1, CH-3012 Bern, Switzerland

ABSTRACT. Scaling properties of kinetic mass conservation equations are presented, and their implications investigated for advective and diffusive transport in an isothermal system in a single spatial dimension. It is demonstrated that for a system undergoing pure advection, scaling the kinetic rate constants by a common factor, thereby preserving their ratios, is equivalent to scaling the time and space coordinates of the original solution. Diffusive transport requires that the diffusion coefficient must also be scaled by the reciprocal factor. These results have far reaching consequences on the possible form of solutions of the kinetic mass transport equations. It follows that the local equilibrium solution, corresponding to the limit as the kinetic rate constants approach infinity, can be extracted from a solution belonging to finite rate constants merely by scaling the time and space coordinates of the kinetic solution. Furthermore the velocities of boundaries of mineral reaction zones must approach their local equilibrium counterparts with increasing time. As a practical consequence, numerical solutions to differential equations representing fluid transport and kinetic reactions of minerals can be validated against solutions to algebraic equations representing conditions of local equilibrium for pure advective transport. Such a test is especially important when attempting to predict the consequences of processes evolving over geologic time spans. The theory is illustrated for a single component system for which an analytical solution exists. A numerical example of weathering is presented for which kinetic and local equilibrium solutions are compared. Finally it is suggested that the recent controversy regarding the discrepancy between laboratory and field derived kinetic rate constants may be a consequence of neglect of the affinity factor in the expression for the reaction rate when applied to field observations. This error can lead to field rate constants that are too small by several orders of magnitude.

* Present address: Southwest Research Institute, Center for Nuclear Waste Regulatory Analyses; 6220 Culebra Road, San Antonio, Texas 78228-0510.

LIST OF SYMBOLS

A_i^{rev}	designation for the ith reversibly reacting aqueous complex.
A_j	designation for the jth primary species.
$\mathbf{A}_m$	affinity of the mth mineral.
$\mathbf{A}_m^{th}$	threshold affinity for the onset of precipitation of the mth mineral.
a	general scale factor applied to the space coordinate.
b	general scale factor applied to the time coordinate.
C_{eq}	equilibrium concentration.
C_i	concentration of the ith reversibly reacting aqueous complex.
C_j	concentration of the jth primary species.
C_l	concentration evaluated at the reaction front l(t).
$C_\pm$	concentration on the downstream and upstream sides of the reaction front for the single component system.
C	solute concentration in the single component system.
C_0	inlet concentration in the single component system.
C_∞	initial concentration in the single component system.
D	diffusion coefficient.
erfc(x)	complementary error function.
F(x, t)	notation for a general function of time and space coordinates.
$f_{\sigma(x,\,t)}$	scaled function f.
F(x, t; {k}, D, u)	general designation for a field variable representing solute concentration or mineral volume fraction.
I_m	net reaction rate of the mth mineral.
K_m	equilibrium constant corresponding to the overall reaction of the mth mineral.
k_m	kinetic rate constant associated with the overall reaction of the mth mineral.
k	kinetic rate constant in the single component system.
{k}	collective set of kinetic rate constants $\{k_1; \ldots; k_M\}$.
K_Δ	distribution coefficient between solid and aqueous phases.
l(t)	reaction front position.
l_m; $l_m^{(i)}$	reaction front corresponding to the mth mineral (for the ith zone boundary).
$\mathscr{M}_m$	designation for the mth mineral.
M	number of reacting minerals.
N	number of primary species.
n_m	number of moles of the mth mineral in a closed system.
Q_m	ion activity product corresponding to the mth mineral.
q	inverse length characterizing the distance for the solute concentration to reach equilibrium.
R	gas constant.

s_m	surface area of the mth mineral per unit volume of bulk rock.
s	solid surface area per unit volume of bulk rock in the single component system.
$T(x, t)$	temperature field at position x and time t.
t	time.
t_σ	scale time.
u	Darcy fluid velocity.
$\overline{V}_m$	molar volume of the mth mineral.
v	average fluid velocity.
v_l	velocity of the lth reaction front.
v_m; $v_m^{(i)}$	reaction front velocity of the mth mineral (at the ith zone boundary).
$W(k, D, u)$	factor in the expression for the equilibration length q for combined advection-diffusion.
x	spatial coordinate.
x_σ	scaled spatial coordinate.
γ_j, γ_i	aqueous activity coefficients for the jth primary species and ith complex.
$\eta(x, t)$	similarity variable for pure diffusive transport.
$\eta_m^{(i)}$	similarity variable for pure diffusive transport for the mth mineral at the ith zone boundary.
$\vartheta(x)$	Heaviside function.
λ	characteristic diffusion length.
ν_{ji}^{aq}	stoichiometric reaction matrix for reversibly reacting aqueous complexes.
ν_{jm}	stoichiometric reaction matrix for mineral reactions.
ξ_m	coefficient varying between zero and one.
σ	scaling parameter.
τ_0	time for mineral to dissolve completely at inlet.
ϕ	porosity.
ϕ_m	volume fraction of the mth mineral.
ϕ_m^∞	initial volume fraction of the mth mineral.
$\phi_s(x, t)$	solid phase volume fraction in the single component system.
ϕ_s^∞	initial solid phase volume fraction in the single component system.
$\chi(l; k)$	quantity in the reaction front velocity in the single component system.
Ψ_j	generalized concentration of the jth primary species in a multicomponent system.
Ψ_j^0	generalized inlet concentration of the jth primary species.
Ω_j	generalized flux of the jth primary species in a multicomponent system.
Ω_j^σ	scaled generalized flux.
$\tilde{(\ )}$	designation for a local equilibrium quantity.

INTRODUCTION

A quantitative time-space description of transport of solute species and their chemical interaction with minerals has the potential of providing a powerful new tool for analyzing many diverse geochemical processes. With the help of the quasi-stationary state approximation it is now possible to carry out numerical calculations of complex geochemical systems evolving over geologic time spans (Lichtner, 1988; Balashov and Lebedeva, 1991; Lichtner, 1991; Lichtner and Biino, 1992; Lichtner and Waber, 1992). However a quantitative description of natural systems often involves many uncertainties associated with initial and boundary conditions, heterogeneities in the flow system, and uncertainties in describing mineral reaction rates. The reaction mechanism of mineral reactions may range from surface to transport controlled depending on the magnitude of the rate constant and the rate of solute transport. As a consequence the reaction rate may be influenced by the geometry of the system resulting from the existence of boundary layers surrounding mineral grains in systems involving a flowing fluid (Murphy, Oelkers, and Lichtner, 1989). Uncertainties arise in incorporating nucleation kinetics and in the lack of a complete understanding of the reaction mechanism and form of the rate law (Steefel and Van Cappellen, 1990). Kinetic rate laws and their associated rate constants are known for only very few minerals for both dissolution and precipitation. An added difficulty in describing mineral reactions is quantifying mineral surface areas and its change with reaction. For example, the surface area of a dissolving mineral may either increase with reaction progress as a result of etch pit formation or decrease as mineral grains dissolve completely. Since the reaction rate is proportional to the surface area, the uncertainty in surface area can lead to substantial uncertainty in predicting the rate of reaction.

This contribution demonstrates that the effects of these uncertainties on solutions to kinetic mass transport equations may not be as significant as previously thought, especially for geochemical processes involving sufficiently long time spans. This is a consequence of the scaling properties of solutions to the kinetic mass transport equations. Scaling the kinetic rate constants by a common factor, which preserves their ratios, is equivalent to scaling the time and space coordinates of the original solution and the diffusion coefficient by the reciprocal factor. This result has far reaching consequences on the possible form of solutions to the kinetic transport equations. Because scaling the time and space coordinates merely stretches or shrinks the spatial profile of the solute concentration or mineral volume fraction without altering its magnitude, the reaction zone sequence and relative maxima and minima are preserved. As the scale factor approaches infinity, it follows that a kinetic solution to the transport equations must yield the same relative maxima and minima for the concentrations of solute species and mineral volume fractions as the corresponding local equilibrium solution. It further follows from the scaling relations that the velocities of propagation of the boundaries of

mineral alteration zones, or reaction fronts, become equal to their local equilibrium counterparts with increasing time under very general circumstances. This result was obtained previously by different methods (Ortoleva and others, 1986; Lichtner, 1988, 1991). Finally, solutions to kinetic transport equations belonging to different *relative* rate constants must scale to the identical local equilibrium solution provided it is unique.

The scaling properties of the kinetic transport equations do not depend on specific models used to describe, for example, the change in surface area or permeability with mineral reaction, provided these relations are scale independent. In this sense the scaling properties are model independent. This observation has important consequences for quantitatively describing mass transport processes in natural systems characterized by large inherent uncertainties.

SCALING PROPERTIES OF KINETIC MASS TRANSPORT EQUATIONS

Scaling relations may place severe restrictions on the time-space behavior of quantities defined through solutions to a system of partial differential equations. Although investigating the properties of solutions to differential equations by scaling the independent variables is a well know technique, it does not appear to have been applied previously to mass transport problems involving mineral precipitation-dissolution reactions. These equations are complicated by the presence of moving boundaries delineating different reaction zones.

Scale Transformation

An example of a scale transformation applied to a function of a single variable is illustrated in figure 1. Scaling the x-coordinate by the constant factor σ leads to the scaled function f_σ defined by

$$f_\sigma(x) = f(\sigma^{-1}x), \tag{1}$$

and therefore the point $\sigma^{-1}\,x$ is transformed to the point x preserving the value of the function f. As is apparent from the figure, the function is stretched or shrunk depending on the size of σ. Shrinking takes place if $\sigma < 1$, and stretching if $\sigma > 1$. Characteristic features of the function f(x) such as discontinuities, relative minima, maxima, and inflection points are all preserved in the scaled function f_σ. Thus, for example, at a relative maximum or minimum x_0, the first derivative of the function f(x) vanishes according to the equation

$$\frac{df}{dx}(x_0) = 0. \tag{2}$$

For the scaled function f_σ it follows that

$$\frac{df_\sigma}{dx}(\sigma x_0) = \sigma^{-1}\frac{df}{dx}(x_0) = 0, \tag{3}$$

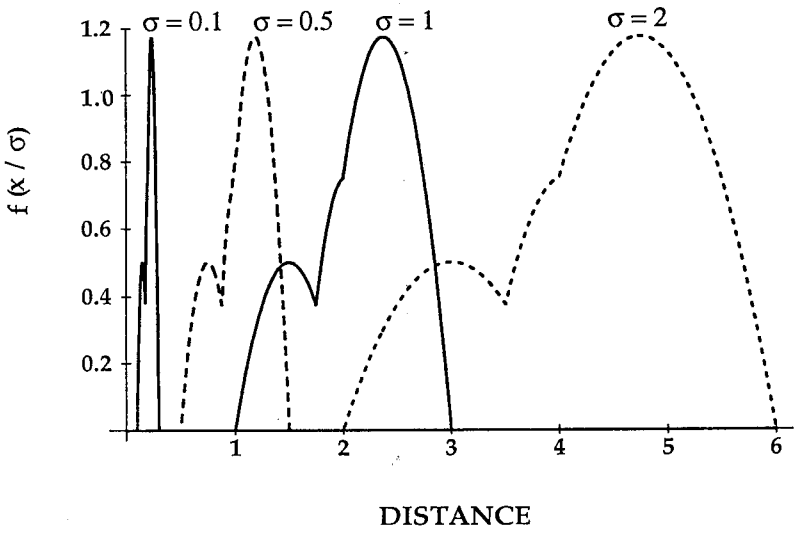

Fig. 1. Scaling transformation applied to a function f(x) of a single variable. Profiles are shown for f(σx) with σ = 0.1, 0.5, 1, and 2.

and therefore the scale transformation preserves the property of a relative maximum or minimum. A similar relation holds for inflection points defined by vanishing of the second derivative.

The scale transformation of the time and space coordinates of the form

$$x_\sigma = \sigma^{-1}x, \tag{4}$$

$$t_\sigma = \sigma^{-1}t, \tag{5}$$

with constant scale factor σ, applied to some function f(x, t) results in the transformed function $f_\sigma(x, t)$ defined by

$$f_\sigma(x, t) = f(x_\sigma, t_\sigma). \tag{6}$$

The inverse transformation is defined by

$$f(x, t) = f_\sigma(\sigma x, \sigma t). \tag{7}$$

The function f may correspond, for example, to field variables such as solute concentrations, mineral volume fractions, temperature, and pressure. As an example, consider the function φ(x, t) defined by the equation

$$\phi(x, t) = \begin{cases} \dfrac{\phi_0}{(v_2 - v_1)t}(v_2 t - x) & (v_1 t \le x \le v_2 t) \\ 0 & \text{otherwise} \end{cases}, \tag{8}$$

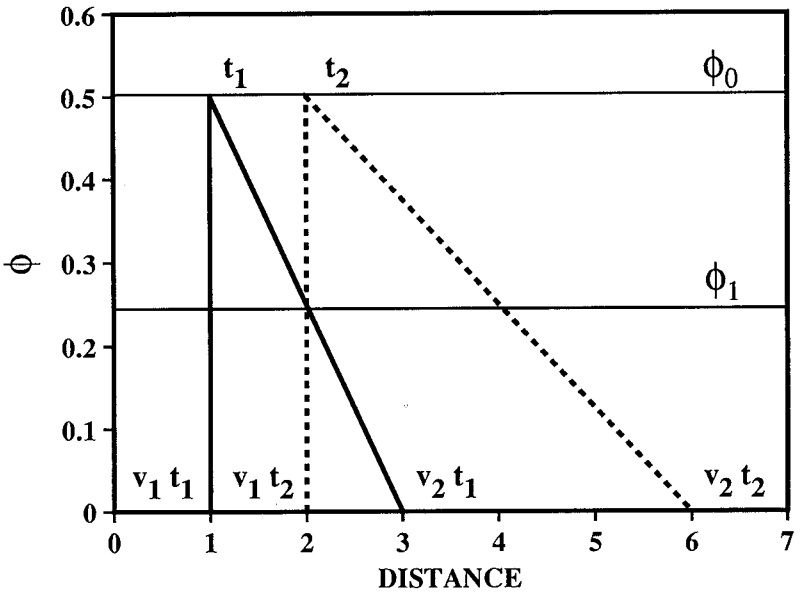

Fig. 2. Illustration of a traveling wave. The traveling wave is invariant under a scale transformation of both the space and time coordinates.

where ϕ_0, v_1, and v_2 are constants. The function $\phi(x, t)$ represents a traveling wave as illustrated in figure 2 for two different times, t_1 and t_2. As defined, clearly ϕ satisfies the scaling relation

$$\phi(\sigma x, \sigma t) = \phi(x, t), \tag{9}$$

and thus is invariant under a scale transformation. Another interesting feature of the function ϕ is the transformation property of the function giving the position of a constant value of ϕ with time. This function, denoted by $l(t)$, is defined implicitly by the relation

$$\phi(l(t), t) = \phi_1 = \text{constant}. \tag{10}$$

It follows that $l(t)$ is given explicitly by the expression

$$l(t) = \left[\left(1 - \frac{\phi_1}{\phi_0}\right) v_2 + \frac{\phi_1}{\phi_0} v_1\right] t. \tag{11}$$

The velocity at which this point moves is given by

$$v_l = \frac{dl}{dt} = \left[\left(1 - \frac{\phi_1}{\phi_0}\right) v_2 + \frac{\phi_1}{\phi_0} v_1\right]. \tag{12}$$

From these relations the scaling properties of $l(t)$ and v_l follow given by the expressions:

$$l(\sigma t) = \sigma l(t), \tag{13}$$

and

$$v_l(\sigma t) = v_l(t) = \text{constant}. \tag{14}$$

This simple example is useful for investigating the scaling properties of chemical reaction fronts as demonstrated below.

Application of the scaling relations to the non-reactive mass transport equation is presented in app. A. In what follows it is assumed that the reader is familiar with the general form of the reactive mass transport equations. Before proceeding to the general case of the transport equations in an open system, first the simpler case of a closed system is considered.

Closed System

The mass transfer equations for a well-mixed, closed system may be expressed in the form

$$\frac{d\Psi_j}{dt} = -\sum_m \nu_{jm} I_m, \tag{15}$$

and

$$\frac{dn_m}{dt} = I_m, \tag{16}$$

for aqueous species and minerals, respectively. In these equations n_m and I_m denote the number of moles and reaction rate, respectively, of the mth mineral, Ψ_j denotes the generalized concentration of the jth primary species with concentration C_j, defined by

$$\Psi_j = C_j + \sum_i \nu_{ji}^{aq} C_i, \tag{17}$$

where the subscript i refers to aqueous complexes with concentration C_i, and ν_{ji}^{aq} refers to the corresponding stoichiometric reaction coefficients. It is assumed that local equilibrium holds within the aqueous phase with the concentrations of aqueous complexes related to concentrations of the primary species by mass action equations. The quantity ν_{jm} denotes the stoichiometric coefficient for reaction of the mth mineral with the aqueous solution. These equations are subject to the initial conditions

$$\Psi_j(0) = \Psi_j^0, \tag{18}$$

and

$$n_m(0) = n_m^0. \tag{19}$$

In a kinetic representation of mineral reactions the reaction rate I_m is specified as some known function of the concentrations of the primary species, which are used to characterize the system. The basic requirement that must be satisfied by the rate law is that the reaction rate tend toward zero as equilibrium is approached. One form for the kinetic rate of mineral reactions consistent with transition state theory (Aagaard and Helgeson, 1982) is given by

$$I_m = -k_m s_m\{1 - \exp[-\mathbf{A}_m/RT]\}, \tag{20}$$

where k_m denotes the kinetic rate constant, s_m denotes the reacting surface area, $\mathbf{A}_m$ denotes the chemical affinity, and R and T denote the gas constant and temperature, respectively. The quantity in curly brackets containing the affinity in the rate expression ensures that the reaction rate vanishes at equilibrium. The rate is taken as positive for precipitation and negative for dissolution, with units of moles per unit volume per unit time. An essential feature of the rate law regarding the scaling properties of the solution is its linear dependence on the kinetic rate constant.

Scaling the time coordinate according to eq (5) leads to the transformed equations

$$\frac{d\Psi_j}{dt_\sigma} = -\sigma \sum_m \nu_{jm} I_m; \tag{21}$$

and

$$\frac{dn_m}{dt_\sigma} = \sigma I_m. \tag{22}$$

Noting that the kinetic rate I_m is proportional to the kinetic rate constants k_m, the scaled equations are identical in form to eqs (15) and (16) if k_m is replaced by σk_m for all reacting minerals. Consequently, because the initial and boundary conditions are invariant under the scale transformation, these equations must have solutions identical to the original equations, and therefore it follows that $\Psi_j(t; \{k\})$ scales with time according to the relation

$$\Psi_j(\sigma^{-1}t; \sigma\{k\}) = \Psi_j(t; \{k\}), \tag{23}$$

with $\sigma\{k\} = \{\sigma k_1, \ldots, \sigma k_M\}$ or, alternatively

$$\Psi_j(t; \sigma\{k\}) = \Psi_j(\sigma t; \{k\}). \tag{24}$$

A similar result holds for the function $n_m(t)$. Therefore if a solution is known for one set of kinetic rate constants, it can be obtained for any other set that preserves their ratios, merely by scaling the time t. Thus the reaction path followed by the system is identical for both sets of rate constants; however, the velocity of the system point as it moves along the path is greater the larger the rate constants. The sequence of secondary

minerals formed, therefore, is also the same, only the times at which they occur along the reaction path are different related by the scale factor.

Changing the relative values of the rate constants leads, in general, to a different reaction path and may involve formation of different secondary minerals. However, because the system is closed, the final equilibrium state of the system is a function only of its initial state and must be independent of the particular reaction path taken by the system and hence the kinetic rate constants.

Open System

In an open system involving advective and diffusive mass transport, the equations describing the system are given by

$$\frac{\partial}{\partial t}(\phi\Psi_j) + \frac{\partial \Omega_j}{\partial x} = -\sum_m \nu_{jm} I_m, \tag{25}$$

for solute species, where Ω_j denotes the generalized flux consisting of contributions from advection and diffusion defined by

$$\Omega_j = -\phi D \frac{\partial \Psi_j}{\partial x} + u\Psi_j, \tag{26}$$

where D denotes the diffusion coefficient considered to be the same for all species, for simplicity, and u designates the Darcy velocity, in general a function of time and distance, and

$$\frac{\partial \phi_m}{\partial t} = \overline{V}_m I_m, \tag{27}$$

for minerals (for more details, see Lichtner, 1985, 1992). These equations are based on a continuum representation of a porous medium. Definitions of the variables used in these equations can be found in the list of symbols.

The transport equations are subject to initial conditions specifying the modal composition of the unreacted rock, the composition of the fluid occupying the pore spaces at t = 0, and boundary conditions specifying the composition of the fluid entering the porous medium at the inlet. The initial fluid composition is specified by the quantity Ψ_j^∞ according to the equation

$$\Psi_j(x, 0) = \Psi_j^\infty, \tag{28}$$

and the initial modal composition of the host rock by ϕ_m^0 according to

$$\phi_m(x, 0) = \phi_m^0. \tag{29}$$

The composition of the fluid at the inlet specified by Ψ_j^0 is defined through the boundary condition

$$\Psi_j(0, t) = \Psi_j^0. \tag{30}$$

Other boundary conditions are also possible, for example, by specifying the fluid flux at the inlet. For the scaling relations to be applicable it is necessary that the initial and boundary conditions remain invariant under a scale transformation, which rules out the flux boundary condition.

Although the positions of the boundaries of the various reaction zones provide convenient quantities with which to describe the system, they do not appear explicitly in the kinetic transport equations. They are, however, implicitly contained in the functions representing the mineral volume fractions. This is in contrast to a local equilibrium description in which the positions of the various reaction fronts are essential variables for describing the system as it evolves in time. In a kinetic description it is possible to define the position of the ith reaction zone boundary corresponding to the mth mineral, denoted by l_m, by the equation

$$\phi_m(l_m(t), t) = \text{constant}. \tag{31}$$

Note that this equation applies to the end points of a reaction zone by taking the constant equal to zero, where the modal abundances vanish as a consequence of the finite rates of reaction. Often, however, a reaction zone is further divided into subzones. At the boundaries of these subzones the modal abundances need not vanish. In a local equilibrium description jump discontinuities occur across the boundaries of the subzones as well as the end points of the zone. However, for each reaction front it is always possible to find at least one mineral for which its modal abundance vanishes. For a non-zero value of the constant, this definition of the position of a reaction front includes fronts contained within a reaction zone, determined by a constant value of the modal composition of some mineral. This definition of a reaction front only holds asymptotically after the system achieves a steady-state, and the front velocities become constant. For diffusive transport under conditions of local equilibrium the mineral modal abundances are rigorously constant at each front for all time starting at $t = 0$ (Lichtner and Balashov, 1992). However, for combined advection and diffusion, in general the mineral modal compositions at the various reaction fronts change with time approaching a constant value asymptotically.

The reaction front velocities are obtained by differentiating the above equation with respect to time to give

$$v_m = -\frac{\partial \phi_m / \partial t}{\partial \phi_m / \partial x}. \tag{32}$$

The front velocities are useful quantities for comparing the rate of weathering of different minerals, for example.

As in a closed system, because the reaction rate I_m of the mth mineral, defined in eq (20), is proportional to the kinetic rate constant k_m, the transport equations are linear in the rate constants. This circumstance leads to significant implications on the possible form of solutions to

the kinetic mass transport equations for rate constants that differ by a constant scale factor. Scaling properties of the kinetic mass transport equations follow directly from eqs (25) and (27). These properties are more complicated than the non-reactive transport equations due to the presence of reaction fronts. Scaling the time and space coordinates by the factor σ according to eqs (4) and (5) leads to the transformed transport equations

$$\frac{\partial}{\partial t_\sigma}(\phi\Psi_j) + \frac{\partial \Omega_j^\sigma}{\partial x_\sigma} = -\sigma \sum_m \nu_{jm} I_m, \tag{33}$$

and

$$\frac{\partial \phi_m}{\partial t_\sigma} = \sigma \bar{V}_m I_m, \tag{34}$$

where the transformed generalized flux Ω_j^σ is defined by

$$\Omega_j^\sigma = -\phi\sigma^{-1} D \frac{\partial \Psi_j}{\partial x_\sigma} + u\Psi_j. \tag{35}$$

Both eqs (33) and (34) have the identical form as the original transport equations given by eqs (25) and (27), if $\{k\}$ is replaced by $\sigma\{k\}$, and D is replaced by σ^{-1} D. Furthermore, both sets of equations are subject to the identical initial and boundary conditions given by eqs (28), (29), and (30) which are invariant under the scale transformation. Therefore a solution to the scaled transport equations is related to the corresponding solution to the original equations according to

$$\Psi_j(x_\sigma, t_\sigma; \sigma\{k\}, \sigma^{-1}D, u) = \Psi_j(x, t; \{k\}, D, u), \tag{36}$$

and

$$\phi_m(x_\sigma, t_\sigma; \sigma\{k\}, \sigma^{-1}D, u) = \phi_m(x, t; \{k\}, D, u), \tag{37}$$

where the functions on the left hand side of these relations are solutions to eqs (33) and (34), and the functions on the right hand side to eqs (25) and (27).

Just as it is possible to deduce the behavior of the solution to the non-reactive transport equation on the diffusion coefficient directly from the scaling relation (see app. A), in this case it is possible, in addition, to investigate the behavior of the solution on the kinetic rate constants. To this end it is convenient to introduce the field variable $F_\alpha(x, t; \{k\}, D, u)$ and rewrite eqs (36) and (37) in the general form

$$F_\alpha(x_\sigma, t_\sigma; \sigma\{k\}, \sigma^{-1}D, u) = F_\alpha(x, t; \{k\}, D, u), \tag{38}$$

where F_α signifies the quantities Ψ_j and ϕ_m. This relation may be expressed in the equivalent form

$$F_\alpha(x, t; \sigma\{k\}, \sigma^{-1}D, u) = F_\alpha(\sigma x, \sigma t; \{k\}, D, u), \tag{39}$$

in which x is replaced by σx and t by σt. Thus scaling the rate constants by a common factor and the diffusion coefficient by the reciprocal factor is equivalent to scaling the time and space coordinates by the same factor. From this equation the behavior of the system for different kinetic rate constants and different diffusion coefficients related by the scale factor σ to the original constants can be deduced. It must be emphasized that in order for the scaling relation to hold, all rate constants must be scaled by the same factor σ. Changing the relative kinetic rate constants in general leads to an entirely different solution with a different sequence of reaction zones. However, as discussed below, for sufficiently long time spans all solutions must tend to the same asymptotically limiting solution, provided it is unique, regardless of the choice of rate constants.

An immediate consequence of eq (39) for a system undergoing pure advective transport is the scaling relation

$$F_\alpha(x, t; \sigma\{k\}, u) = F_\alpha(\sigma x, \sigma t;\{k\}, u). \tag{40}$$

Thus scaling the time and space coordinates by a common factor is equivalent to scaling the kinetic rate constants by the same factor. Note that no assumptions are made regarding the particular models that may be used to represent mineral surface area, porosity, or permeability. They may be described by any scale invariant function of the mineral volume fractions, for example. Hence in this sense the scaling relations are model independent.

Zone boundary positions and reaction front velocities.—From the scaling relation satisfied by the mineral volume fraction, it is possible to derive scaling properties for the positions of the reaction zone boundaries or reaction fronts and their velocities. The position of the ith reaction front corresponding to the mth mineral, $l_m^{(i)}(t; \{k\}, D, u)$, is defined implicitly by the relation

$$\phi_m(l_m^{(i)}(t; \{k\}, D, u), t; \{k\}, D, u) = \text{constant}, \tag{41}$$

according to eq (31). Likewise the position of the reaction front, $l_m^{(i)}(t; \sigma\{k\}, \sigma^{-1}D, u)$, corresponding to the scaled transport equations satisfies a similar equation

$$\phi_m(l_m^{(i)}(t; \sigma\{k\}, \sigma^{-1}D, u), t; \sigma\{k\}, \sigma^{-1} D, u) = \text{constant}. \tag{42}$$

Making use of the scaling properties of ϕ_m, the latter relation can be expressed as

$$\phi_m(\sigma l_m^{(i)}(t; \sigma\{k\}, \sigma^{-1}D, u), \sigma t; \{k\}, D, u) = \text{constant}. \tag{43}$$

Note that in this expression l_m is evaluated at time t and not σt. Comparing this equation with eq (41) in which t is replaced by σt leads to the scaling relation for the reaction zone boundaries:

$$\sigma l_m^{(i)}(t; \sigma\{k\},\sigma^{-1}D, u) = l_m^{(i)}(\sigma t; \{k\}, D, u). \tag{44}$$

This relation is analogous to the transformation of the spatial coordinate x. Thus the position of the reaction front at time σt, corresponding to rate constants $\{k\}$ and diffusion coefficient D, is equal to σ times the position of the front at time t corresponding to the scaled rate constants $\sigma\{k\}$ and diffusion coefficient σ^{-1} D.

The scaling relation for the reaction front velocities follows from the definition

$$v_m^{(i)}(t; \{k\}, D, u) = \frac{d}{dt} l_m^{(i)}(t; \{k\}, D, u). \tag{45}$$

Differentiating both sides of eq (44) with respect to time yields the scaling relation

$$v_m^{(i)}(t; \sigma\{k\}, \sigma^{-1}D, u) = v_m^{(i)}(\sigma t; \{k\}, D, u), \tag{46}$$

in which the scaling factor σ cancels. According to this result by scaling the time coordinate the velocities of the zone boundaries are related to the velocities corresponding to the solution with scaled rate constants $\sigma\{k\}$ and diffusion coefficient σ^{-1} D at time t.

Local Equilibrium Limit

A solution to the kinetic transport equations approaches the local equilibrium limiting solution as the rate constants grow without bound according to the relation:

$$\lim_{\{k\}\to\infty} F_\alpha(x, t; \{k\}, D, u) \to \tilde{F}_\alpha(x, t; D, u), \tag{47}$$

where $\tilde{F}_\alpha(x, t; D, u)$ designates field variables corresponding to conditions of local equilibrium as defined in app. B. By simultaneously considering the limit in which $\{k\} \to \infty$ and $D \to 0$, the pure advective local equilibrium limit is obtained:

$$\lim_{\substack{\{k\}\to\infty \\ D\to 0}} F_\alpha(x, t; \{k\}, D, u) \to \tilde{F}_a(x, t; u). \tag{48}$$

These relations may be taken as the definition of the local equilibrium limit.

To investigate the implications of the scaling properties on the relation between the kinetic solution and the local equilibrium limiting solution, consider the limit $\sigma \to \infty$ applied to eq (39). The right hand side of this equation tends, by definition, to the local equilibrium limit corresponding to pure advective transport as follows from eq (48). Therefore by scaling the time and space coordinates of the kinetic solution $F_\alpha(x, t; \{k\}, D, u)$ corresponding to fixed rate constants $\{k\}$, the kinetic solution can be made to approach arbitrarily close to the pure advective local equilibrium limiting solution according to

$$\lim_{\sigma\to\infty} F_\alpha(\sigma x, \sigma t; \{k\}, D, u) = \lim_{\sigma\to\infty} F_\alpha(x, t; \sigma\{k\}, \sigma^{-1}D, u) \to \tilde{F}_i(x, t; u). \tag{49}$$

The reaction zone boundaries and velocities also approach their limiting values corresponding to the pure advective local equilibrium limit:

$$\lim_{\sigma\to\infty} \frac{1}{\sigma} l_m^{(i)}(\sigma t; \{k\}, D, u) = \lim_{\sigma\to\infty} l_m^{(i)}(t; \sigma\{k\}, \sigma^{-1}D, u) \to \tilde{l}_m^{(i)}(t; u), \qquad (50)$$

and

$$\lim_{\sigma\to\infty} v_m^{(i)}(\sigma t; \{k\}, D, u) = \lim_{\sigma\to\infty} v_m^{(i)}(t; \sigma\{k\}, \sigma^{-1} D, u) \to \tilde{v}_m^{(i)}. \qquad (51)$$

These relations are of fundamental importance. They imply that after a sufficient amount of time has elapsed the profiles of the solute concentration and mineral volume fraction obtained from the kinetic transport equations bear a strong resemblance to the corresponding local equilibrium solution. Merely by scaling both the time and space coordinates of the kinetic solution, it is possible to extract the local equilibrium limiting solution for any arbitrary set of rate constants. A scale transformation of the spatial coordinate does not change the amplitude of the solute concentration or mineral volume fraction but only stretches or shrinks the spatial profile. Therefore given a sufficiently long time span, a kinetic solution belonging to finite rate constants preserves maxima and minima of the corresponding local equilibrium solution. The widths of the various reaction zones and the shapes of the concentration and volume fraction profiles, however, are different in the kinetic solution.

In an isothermal system the solution to the kinetic transport equations approaches asymptotically a steady-state in which the various reaction zones propagate with constant velocity. The local equilibrium velocities $\tilde{v}_m^{(i)}$ corresponding to pure advective transport in an isothermal system are also independent of time as are the solute concentrations and mineral modal abundances within each reaction zone. Therefore it follows from eq (51) that if $\tilde{v}_m^{(i)}$ obtained from a kinetic solution is also constant independent of the time, it must be identical to the local equilibrium limiting value $\tilde{v}_m^{(i)}$. Thus the reaction front velocities in a kinetic description approach asymptotically the local equilibrium limiting values. This result has been obtained previously using different methods by Ortoleva and others (1986) and Lichtner (1988).

The asymptotic solution to the kinetic transport equations may be depicted as a traveling wave which does not change shape in the vicinity of each reaction front. The velocity of the ith reaction front $l_i(t)$ in the traveling wave approximation is given by Lichtner (1988)

$$v_i = \frac{dl_i}{dt} = \frac{\langle \Omega_j \rangle_i}{\langle \phi \Psi_j \rangle_i + \sum \nu_{jm} \bar{V}_m^{-1} \langle \phi_m \rangle_i}. \qquad (52)$$

In this equation the angular brackets $\langle \ldots \rangle_i$ denote the difference in the enclosed quantity across the ith reaction front. If the solute concentration comes to equilibrium with the minerals on either side of the front, this

expression reduces to the Rankine-Hugoniot equations, and the velocities of the fronts are identical to that obtained from local equilibrium considerations. Normally reaction zones increase in width at a constant velocity. Special zones, referred to as ghost zones, have a constant width and are governed by diffusive transport (Lichtner and Balashov, 1992). In a local equilibrium description their width approaches zero in the limit as the diffusion coefficient tends to zero.

Sensitivity of the solution to kinetic rate constants.—As demonstrated above, a solution to the kinetic transport equations for a finite set of rate constants {k} can be made to approach as closely as desired to the local equilibrium limiting solution corresponding to pure advective transport by scaling the time and space coordinates. Since this statement is true regardless of the choice of rate constants {k}, it further follows that two solutions with the same initial and boundary conditions but corresponding to different sets of kinetic rate constants must scale to the same local equilibrium limiting solution. This is true provided the local equilibrium solution is unique. In addition the sequence of reaction zones in the steady-state limit must be the same as determined from the corresponding local equilibrium solution. Thus altering the kinetic rate constants cannot affect the reaction zone sequence. From these results it can be concluded that for sufficiently large time spans kinetics plays a minor role in determining the behavior of the system.

It should be kept in mind, however, that a solution corresponding to finite rate constants {k} does *not* strictly approach the local equilibrium solution with increasing time. Rather only the kinetic solution scaled in both the time and space coordinate approaches arbitrarily close to the local equilibrium solution as the scale factor tends to infinity. However, the interior region of a reaction zone approaches the local equilibrium limit more rapidly than the region in the neighborhood of a reaction front.

Pure Diffusion

So far the discussion has focused on transport involving both advection and diffusion. Similar results can be derived for pure diffusive transport. In this case it is useful to consider a slightly different scale transformation of the form (Balashov and Lebedeva, 1991)

$$x_\sigma = x/\sqrt{\sigma}, \tag{53}$$

and

$$t_\sigma = t/\sigma. \tag{54}$$

As pointed out by Balashov (private communication), this relation may be derived by considering the more general transformation:

$$x' = ax, \tag{55}$$

and

$$t' = bt, \tag{56}$$

where a and b are arbitrary real numbers. Solutions to the combined advection and diffusion kinetic transport equations then scale according to

$$F(ax, bt; \{k\}, D, u) = F(x, t; b^{-1}\{k\}, a^2b^{-1}D, ab^{-1}u). \tag{57}$$

The previous transformation defined by eqs (4) and (5) is obtained by demanding that the coefficient multiplying u be unity, or

$$\sigma^{-1} = a = b. \tag{58}$$

The transformation for pure diffusive transport given by eqs (53) and (54) follows from the condition

$$b = a^2, \tag{59}$$

giving unit coefficient multiplying D. With this transformation solutions to the pure diffusion kinetic transport equations scale according to

$$F_\alpha(\sqrt{\sigma}x, \sigma t; \{k\}, D) = F_\alpha(x, t; \sigma\{k\}, D), \tag{60}$$

in which the diffusion coefficient remains unchanged. The reaction zone boundaries and reaction front velocities satisfy the relations

$$\frac{1}{\sqrt{\sigma}} l_m^{(i)}(\sigma t; \{k\}, D) = l_m^{(i)}(t; \sigma\{k\}, D), \tag{61}$$

and

$$\sqrt{\sigma} v_m^{(i)}(\sigma t; \{k\}, D) = v_m^{(i)}(t; \sigma\{k\}, D). \tag{62}$$

Under the scale transformation given by eqs (53) and (54), the local equilibrium limiting solution has the property that it is invariant:

$$\tilde{F}_\alpha(\sqrt{\sigma}x, \sigma t; D) = \tilde{F}_\alpha(x, t; D). \tag{63}$$

This result implies that the pure diffusion moving boundary problem can be described in terms of a single variable η, referred to as the Stefan variable, defined by

$$\eta(x, t) = \frac{x}{2\sqrt{Dt}}. \tag{64}$$

This result has been used by Novak, Schechter, and Lake (1989) to obtain solutions for pure diffusion. The positions of reaction fronts are given by

$$\tilde{l}_m^{(i)} = 2\eta_m^{(i)}\sqrt{Dt}, \tag{65}$$

with the corresponding velocities

$$\tilde{v}_m^{(i)} = \eta_m^{(i)} \sqrt{\frac{D}{t}}, \tag{66}$$

for constants $\eta_m^{(i)}$. These quantities are not invariant but scale according to the relations

$$\frac{1}{\sqrt{\sigma}} \tilde{l}_m^{(i)}(\sigma t; D) = \tilde{l}_m^{(i)}(t; D), \tag{67}$$

and

$$\sqrt{\sigma} \tilde{v}_m^{(i)}(\sigma t; D) = \tilde{v}_m^{(i)}(t; D), \tag{68}$$

similar to the kinetic case.

From the scaling relations it follows that the limit of the kinetic solution as $\sigma \to \infty$ approaches the corresponding local equilibrium solution according to

$$\lim_{\sigma\to\infty} F_\alpha(\sqrt{\sigma}x, \sigma t; \{k\}, D) = \lim_{\sigma\to\infty} F_\alpha(x, t; \sigma\{k\}, D) \to \tilde{F}_\alpha(x, t; D). \tag{69}$$

Likewise the reaction front positions and velocities approach the corresponding local equilibrium limit. For example it follows that

$$\lim_{\sigma\to\infty} \frac{l_m^{(i)}(\sigma t; \{k\}, D)}{\tilde{l}_m^{(i)}(\sigma t; D)} = \lim_{\sigma\to\infty} \frac{l_m^{(i)}(t; \sigma\{k\}, D)}{\tilde{l}_m^{(i)}(t; D)} = 1, \tag{70}$$

with a similar result for the reaction front velocities.

EXAMPLES

In this section several examples are presented illustrating the scaling properties of the kinetic mass transport equations. The relation between solutions based on a kinetic description of mineral reaction rates and the corresponding local equilibrium limit are investigated.

Single Component System

The first example considers a single component system. As a fluid undersaturated with respect to a solid phase infiltrates or diffuses into a porous column containing the solid, the solid dissolves producing a reaction front l(t) that advances with time in the direction of flow. The problem is to determine the position of the dissolution front as a function of time and the concentration profile of the solute species and modal composition of the solid as functions of time and distance.

For the simple system involving the reaction of a single component mineral such as quartz according to a linear rate law, an analytic solution to the transport equations exists based on the quasi-stationary state

approximation assuming constant porosity, permeability, and mineral surface area (Lichtner, 1988). In this approximation the partial time derivative contained in the transient solute transport equations is neglected. The transport equations take the form

$$\phi D \frac{d^2C}{dx^2} - u \frac{dC}{dx} = ks(C - C_{eq})\theta(x - l(t)), \tag{71}$$

for the solute species, and

$$\frac{\partial \phi_s}{\partial t} = ks\overline{V}_s(C - C_{eq})\theta(x - l(t)), \tag{72}$$

for the solid phase, where C denotes the solute concentration, k denotes the kinetic rate constant, s denotes the specific surface area, C_{eq} denotes the equilibrium concentration, and ϕ_s and $\overline{V}_s$ denote the volume fraction and molar volume of the solid phase, respectively. The function $\theta(x)$ denotes the Heaviside function equal to one if $x \geq 0$, and zero otherwise. The position of the dissolution front is denoted by l(t). These equations are solved subject to the initial and boundary conditons

$$C(0, t) = C_0, \tag{73}$$

and

$$\phi_s(x, 0) = \phi_s^\infty, \tag{74}$$

determining the inlet fluid composition and initial solid modal composition, respectively. The moving boundary problem posed by these equations requires determining the solute concentration C(x, t; k, D, u), mineral volume fraction ϕ_s(x, t; k, D, u), and position of the dissolution front l(t; k, D, u). The solution to these equations is given in app. C.

The scaling properties of the quartz dissolution front determined from eq (C.26) is illustrated in figure 3 where the reaction front position is plotted as a function of time for σ = 1, 2, and 10. Also shown in the figure is the local equilibrium limit for pure advection (dashed-dotted line) and combined advection and diffusion. For this example $k = 10^{-10}$ moles $cm^{-2}\,s^{-1}$, $s = 1\ cm^{-1}$, $D = 5 \times 10^{-4}\ cm^2\,s^{-1}$, $u = 1\ m\,y^{-1}$, $C_{eq} = 10^{-3}$ moles $liter^{-1}$, $\phi_s^\infty = 0.9$, and $C_0 = 0$. The values for k, s, and C_{eq} correspond approximately to the dissolution of quartz at 100°C for a grain size of 1 mm. As time increases the front velocities become constant approaching the pure advective local equilibrium limit, with the positions of the fronts displaced by the characteristic diffusion length $\lambda = \phi D/u \simeq 15$ cm. As σ increases, the position of the front described by the kinetic formulation approaches the pure advective local equilibrium result. The thin dashed lines illustrate the scaling relation

$$l(2t; k, D) = 2l(t; 2k, D/2), \tag{75}$$

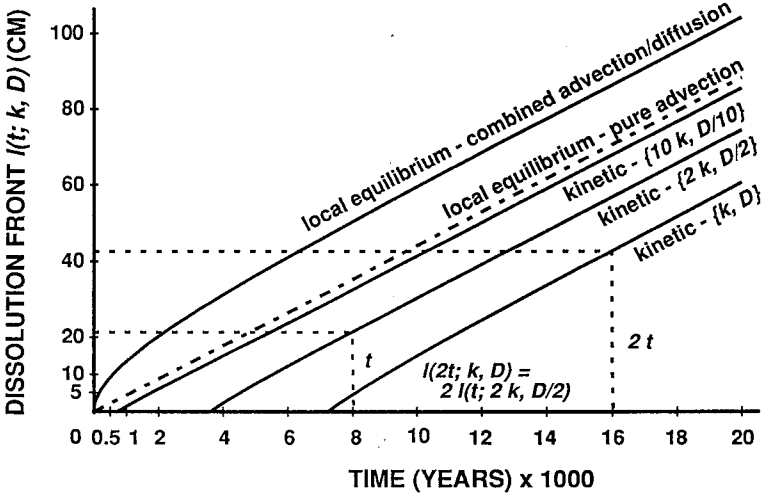

Fig. 3. Scaling properties of the dissolution front l(t; k, D, u) illustrated for a single component system. The position of the reaction front in centimeters is plotted as a function of time in years for kinetic and local equilibrium solutions to the transport equations. In addition the local equilibrium limit for combined advection and diffusion and pure advection (dashed-dotted line) are also shown.

showing the correspondence between the dissolution fronts with a scaling factor $\sigma = 2$ at times t = 8000 and 16,000 yrs.

Shown in figures 4 and 5 are the results of scaling the solute concentration and volume fraction defined by eqs (C.1) and (C.2), respectively. Both quantities are plotted as a function of distance for an elapsed time of 16,000 yrs with the origin of the coordinate system taken to coincide with the instantaneous position of the dissolution front. The solid line labeled $\sigma = \infty$ in figure 4 corresponds to the local equilibrium limit. At the reaction front the solute concentration is approximately constant as can be seen from the figure. The concentration decreases toward the inlet as a consequence of diffusive transport. As is apparent from the figures, with increasing σ the solution to the kinetic transport equations approaches the local equilibrium limit. It should be emphasized, however, that with increasing time for a fixed kinetic rate constant, the kinetic solution to the transport equations approaches a steady-state limit, given by the curves labeled $\sigma = 1$, which clearly does not correspond to the local equilibrium solution. Only by scaling both the time and space coordinates can the local equilibrium solution be extracted from the kinetic solution.

Application to Weathering

This section considers weathering of a hydrothermally altered phonolite host rock found in the Poços de Caldas alkaline complex. This

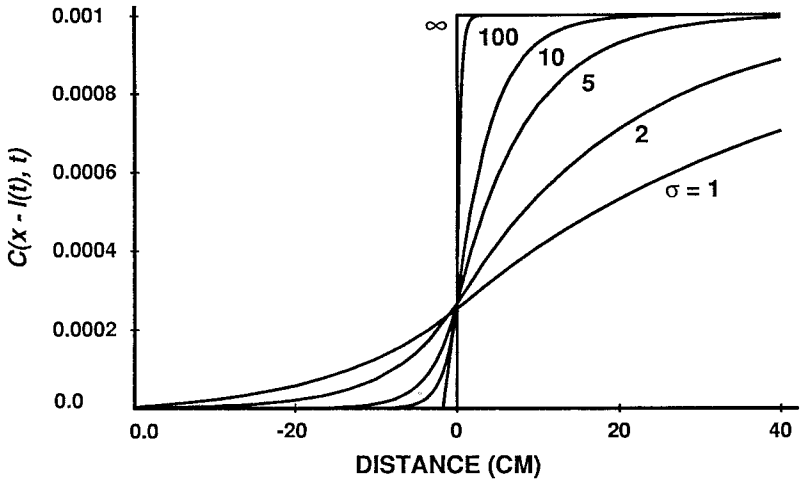

Fig. 4. Solute concentration C(x, t; σk, σ^{-1}D, u) plotted for t = 250 yrs as a function of distance relative to the instantaneous position of the dissolution front l(t; σk, σ^{-1}D, u) for scale factors σ = 1, 2, 5, 10, 100, and ∞. The local equilibrium solution corresponds to σ = ∞. The curves are calculated for the same conditions as in the previous figure. Note that the solute concentration at the reaction front becomes independent of the scaling factor as σ increases.

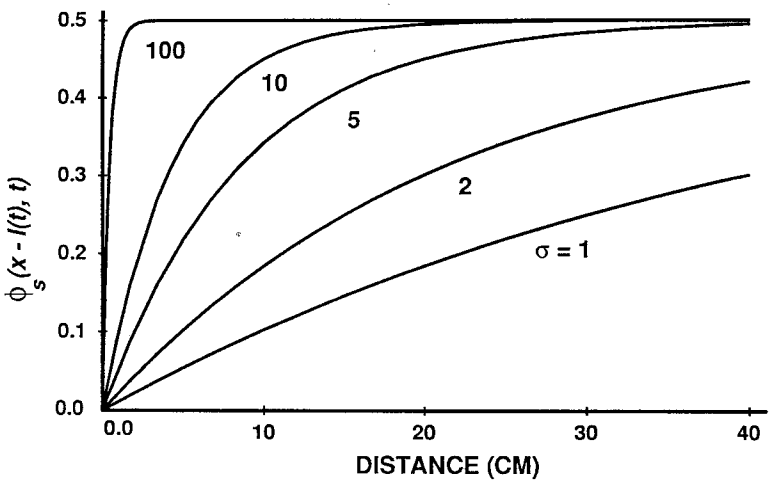

Fig. 5. Volume fraction plotted as a function of distance relative to the dissolution front for the same conditions as figure 3.

problem was considered previously as part of an international natural analogue project on the transport of uranium (Lichtner and Waber, 1992). There it was demonstrated that qualitative agreement with field observations conducted by Waber (ms) could be obtained by considering downward percolation of rainwater through a host rock consisting of the minerals K-feldspar, kaolinite, illite (as muscovite), and fluorite. In this work this example is used to illustrate the scaling properties of the kinetic transport equations.

This system is assumed to be described in terms of 9 primary species consisting of K^+, Na^+, Ca^{2+}, Al^{3+}, H^+, SiO_2, F^-, HCO_3^-, and Cl^-. Both Na^+ and Cl^- are inert but are included to describe the composition of the infiltrating rainwater. Thermodynamic data used in the calculation, with the exception of illite, were taken from the EQ3/6 database. The qualitative features of the resulting weathering profile are extremely sensitive to the value used for the illite log K. In this work a log K of -9.5 was chosen compared to the value of -11.02 for muscovite in the EQ3/6 database. The latter value was found to produce geologically unreasonable results resulting in the precipitation of large amounts of K-feldspar. The value used in the present work, however, does not result in as good a fit to field observations as the value of -10.4 used in Lichtner and Waber (1992). In that case, however, illite appears as a ghost zone requiring special considerations to obtain a proper solution (Lichtner and Balashov, 1992).

First the situation represented by local chemical equilibrium is considered. This results in a set of algebraic equations to determine the solute concentrations, mineral volume fractions, and reaction front velocities. The results of reaction of percolating rainwater through the hydrothermally altered phonolite host rock are presented in table 1. The details of the calculation may be found in Lichtner (1991). Here it is noted that the local equilibrium equations do not determine the sequence of reaction zones directly but only by trial and error methods involving iterating the zone sequence until a consistent solution is obtained. Five distinct alteration zones were found resulting in the zone sequence:

$$\mathrm{F|Gbs|Gbs - Kln|Ill|Kfs - Ill|Kfs - Ill - Fl|Kfs - Ill - Kln - Fl,}$$

where F denotes a zone consisting of fluid only with the composition of the infiltrating fluid. Note that kaolinite forms two distinct reaction zones: a zone at the top of the weathered column consisting of both primary and secondary kaolinite and primary kaolinite deeper in the profile.

Presented in table 1 are the pH, P_{CO_2}, concentrations for primary species, generalized concentrations Ψ_j and aqueous complexes, and mineral volume fractions for each reaction zone beginning with the inlet and ending with the unaltered host rock. The bottom two rows give the porosity ϕ and velocities of the various reaction fronts relative to the Darcy velocity v_0, respectively. The inlet fluid is taken as rainwater

TABLE 1

Results of a local equilibrium calculation with the identical inlet fluid composition and initial host rock composition as used in the corresponding kinetic calculation shown in figures 6 and 7. For sufficiently long elapsed time spans, the results show excellent agreement with the corresponding kinetic calculations

	inlet	zone 1	zone 2	zone 3	zone 4	zone 5	zone 6
pH	4.30	4.32	4.32	5.75	6.75	6.75	5.82
log P_{CO_2}	−2.00	−2.00	−2.00	−2.10	−2.55	−2.56	−2.11
				primary species			
K^+	1.00×10^{-5}	1.00×10^{-5}	1.00×10^{-5}	1.26×10^{-4}	3.06×10^{-4}	3.07×10^{-4}	1.11×10^{-4}
Na^+	2.74×10^{-5}	2.74×10^{-5}	2.74×10^{-5}	2.74×10^{-5}	2.74×10^{-5}	2.74×10^{-5}	2.74×10^{-5}
Ca^{2+}	5.00×10^{-6}	5.00×10^{-6}	5.00×10^{-6}	5.00×10^{-6}	4.99×10^{-6}	3.10×10^{-4}	3.18×10^{-4}
Al^{3+}	8.24×10^{-11}	7.55×10^{-7}	7.55×10^{-7}	3.93×10^{-11}	1.36×10^{-15}	1.60×10^{-15}	9.81×10^{-13}
$SiO_2(aq)$	1.00×10^{-6}	1.00×10^{-6}	5.68×10^{-5}	5.68×10^{-5}	5.95×10^{-4}	5.99×10^{-4}	1.72×10^{-3}
HCO_3^-	3.10×10^{-6}	3.25×10^{-6}	3.25×10^{-6}	7.07×10^{-5}	2.48×10^{-4}	2.48×10^{-4}	8.11×10^{-5}
F^-	1.00×10^{-10}	9.99×10^{-11}	9.99×10^{-11}	1.00×10^{-10}	1.00×10^{-10}	6.12×10^{-4}	6.00×10^{-4}
Cl^-	9.50×10^{-5}	9.50×10^{-5}	9.50×10^{-5}	9.50×10^{-5}	9.50×10^{-5}	9.50×10^{-5}	9.50×10^{-5}
				Ψ_j			
K^+	1.00×10^{-5}	1.00×10^{-5}	1.00×10^{-5}	1.26×10^{-4}	3.06×10^{-4}	3.07×10^{-4}	1.11×10^{-4}
Na^+	2.74×10^{-5}	2.74×10^{-5}	2.74×10^{-5}	2.74×10^{-5}	2.74×10^{-5}	2.74×10^{-5}	2.74×10^{-5}
Ca^{2+}	5.00×10^{-6}	5.00×10^{-6}	5.00×10^{-6}	5.00×10^{-6}	5.00×10^{-6}	3.12×10^{-4}	3.19×10^{-4}
Al^{3+}	1.00×10^{-10}	9.25×10^{-7}	9.25×10^{-7}	1.79×10^{-9}	9.28×10^{-11}	1.52×10^{-8}	8.94×10^{-6}
$SiO_2(aq)$	1.00×10^{-6}	1.00×10^{-6}	5.68×10^{-5}	5.68×10^{-5}	5.96×10^{-4}	6.00×10^{-4}	1.72×10^{-3}
HCO_3^-	3.43×10^{-4}	3.43×10^{-4}	3.43×10^{-4}	3.43×10^{-4}	3.43×10^{-4}	3.43×10^{-4}	3.43×10^{-4}
F^-	1.00×10^{-10}	1.00×10^{-10}	1.00×10^{-10}	1.00×10^{-10}	1.00×10^{-10}	6.13×10^{-4}	6.28×10^{-4}
Cl^-	9.50×10^{-5}	9.50×10^{-5}	9.50×10^{-5}	9.50×10^{-5}	9.50×10^{-5}	9.50×10^{-5}	9.50×10^{-5}
				aqueous complexes			
$AlOH^{2+}$	1.51×10^{-11}	1.46×10^{-7}	1.46×10^{-7}	2.02×10^{-10}	6.80×10^{-14}	7.37×10^{-14}	5.34×10^{-12}
$Al(OH)_2^+$	2.38×10^{-12}	2.40×10^{-8}	2.40×10^{-8}	8.92×10^{-10}	2.96×10^{-12}	3.03×10^{-12}	2.58×10^{-11}
$Al(OH)_3(aq)$	4.10×10^{-14}	4.35×10^{-10}	4.35×10^{-10}	4.35×10^{-10}	1.44×10^{-11}	1.44×10^{-11}	1.44×10^{-11}
$Al(OH)_4^-$	7.50×10^{-16}	8.35×10^{-12}	8.35×10^{-12}	2.26×10^{-10}	7.54×10^{-11}	7.65×10^{-11}	8.92×10^{-12}
AlF_2^+	2.92×10^{-18}	2.67×10^{-14}	2.67×10^{-14}	1.35×10^{-18}	4.40×10^{-23}	1.64×10^{-9}	9.86×10^{-7}
$AlF_3(aq)$	3.59×10^{-24}	3.28×10^{-20}	3.28×10^{-20}	1.65×10^{-24}	5.31×10^{-29}	1.17×10^{-8}	6.91×10^{-6}
AlF_4^-	9.03×10^{-32}	8.23×10^{-28}	8.23×10^{-28}	4.14×10^{-32}	1.33×10^{-36}	1.79×10^{-9}	1.04×10^{-6}
$H_3SiO_4^-$	3.11×10^{-12}	3.27×10^{-12}	1.86×10^{-10}	5.04×10^{-9}	5.32×10^{-7}	5.44×10^{-7}	1.82×10^{-7}
CO_3^{2-}	3.00×10^{-12}	3.31×10^{-12}	3.31×10^{-12}	1.96×10^{-9}	7.03×10^{-8}	7.41×10^{-8}	2.81×10^{-9}
$CO_2(aq)$	3.40×10^{-4}	3.39×10^{-4}	3.39×10^{-4}	2.72×10^{-4}	9.46×10^{-5}	9.34×10^{-5}	2.61×10^{-4}
CaF^+	2.28×10^{-15}	2.28×10^{-15}	2.28×10^{-15}	2.25×10^{-15}	2.19×10^{-15}	7.77×10^{-7}	7.89×10^{-7}
$CaCO_3(aq)$	2.90×10^{-14}	3.19×10^{-14}	3.19×10^{-14}	1.84×10^{-11}	6.27×10^{-10}	3.56×10^{-8}	1.41×10^{-9}
				mineral modal abundances			
$\phi_{gibbsite}$		0.3751	9.9313×10^{-4}	0.	0.	0.	0.
$\phi_{kaolinite}$		0.	0.5826	0.	0.	0.	0.1500
$\phi_{k-feldspar}$		0.	0.	0.	0.4920	0.4934	0.6000
ϕ_{illite}		0.	0.	0.5491	0.3372	0.3366	0.1500
$\phi_{fluorite}$		0.	0.	0.	0.	4.9685×10^{-2}	5.0000×10^{-2}
ϕ		0.6249	0.4164	0.4509	0.1708	0.1204	5.0000×10^{-2}
v/v_0		7.876×10^{-8}	4.768×10^{-6}	2.985×10^{-5}	5.963×10^{-5}	1.514×10^{-4}	5.674×10^{-4}

adjusted for infiltration through a soil zone at the top of the weathered profile with the composition given in the column labeled inlet in table 1. The inlet concentration of the chloride ion is calculated by charge balance assuming values for the other species given in table 1 with an assumed pH of 4.3 and a log P_{CO_2} of −2. The unweathered host rock is represented as a homogeneous porous medium with the modal composition given in the column labeled zone 6 in table 1 consisting of minerals K-feldspar, illite (muscovite), kaolinite, and fluorite.

According to table 1 the pH jumps from its initial value of 4.3 to 5.75 across the gibbsite-kaolinite | illite reaction front as illite dissolves producing kaolinite and gibbsite. It jumps again to 6.75 across the illite | K-feldspar-illite reaction front as K-feldspar dissolves producing illite. The pH drops to approx 5.8 as the fluid comes to equilibrium with the hydrothermally altered phonolite host rock. The steep rise in the pH from approx 4.3 to 6.75 represents a hydrolytic front at which K-feldspar and illite dissolve, and kaolinite and gibbsite precipitate. The dominate aluminum species in the zones with fluoride present consist of the fluoride complexes AlF_3 and AlF_4^-.

Next the solution to the kinetic mass transport equations is considered. Kinetic calculations are based on the quasi-stationary state approximation taking into account kinetics of both mineral precipitation and dissolution reactions (Lichtner, 1988). Further details of the method of calculation may be found in Lichtner (1992). The kinetic rate constants and surface areas used in the calculation are listed in table 2. For K-feldspar the rate law is taken from Helgeson, Murphy, and Aagaard (1984). Illite is taken to have the same rate constant as K-feldspar but with a surface area 20 times smaller. A reference Darcy velocity of 1 m y^{-1} is used in the calculations.

Shown in figure 6 is the resulting volume fraction profile plotted as a function of distance for elapsed times of 2 my. Gibbsite along with secondary kaolinite and illite appear as alteration products during weathering as K-feldspar, fluorite, primary kaolinite, and illite dissolve. The qualitative features of the weathered profile and comparison with field observations are presented by Lichtner and Waber (1992). A thick, high porosity, kaolinite zone forms near the surface consisting of both primary and secondary kaolinite, followed by a dissolution front of primary kaolinite deeper in the profile. Both gibbsite and illite form bi-modal distributions. A plateau occurs in the K-feldspar profile with a gradual increase in modal abundance with depth approaching the value in the unweathered rock. The general features of these zones are in qualitative agreement with field observations.

Shown in figure 7A is the kinetic result for the mineral volume fractions corresponding to an elapsed time of 100,000 yrs plotted as a

TABLE 2

Kinetic rate constants k_m *and initial surface areas* s_m *used in the kinetic calculations*

Mineral	k (moles $cm^{-2}sec^{-1}$)	s (cm^{-1})
K-feldspar	3.16×10^{-16}	10.0
illite	3.16×10^{-16}	0.5
kaolinite	1.0×10^{-17}	45.0
gibbsite	$1. \times 10^{-16}$	5.0
fluorite	$1. \times 10^{-15}$	1.0

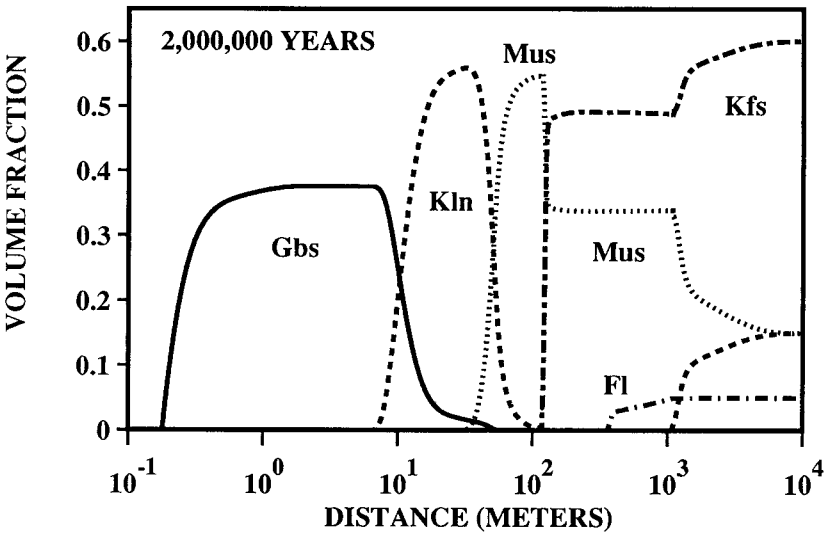

Fig. 6. Mineral modal abundances corresponding to the weathering of a hydrothermally altered phonolite host rock plotted as a function of depth after elapsed time of 2 my. The inlet water percolating through the top of the weathered column has the composition given in the first column in table 1.

function of distance. In figure 7B the local equilibrium result given in table 1 is compared with the kinetic result corresponding to 2 my scaled by a factor of 20 to a time of 100,00 yrs. Comparing figures 7A with B clearly demonstrates that the local equilibrium solution is very different from the kinetic solution for early enough times. Nevertheless as figure 7B demonstrates, by scaling the kinetic solution it can be made to approach arbitrarily close to the local equilibrium result. The major difference is the smooth profile obtained in the kinetic case compared to the sharp reaction front in the local equilibrium result. Notice that all reaction zones with the exception of the kaolinite zone near the surface agree remarkably well with the local equilibrium values. The volume fraction of kaolinite in this zone, however, is still increasing with time. To obtain better agreement a larger scale factor would be necessary.

The concentration profiles of solute species K^+, total Al, SiO_2, and the pH are compared in figure 8 between the scaled kinetic solution and local equilibrium. Excellent agreement exists between the scaled kinetic concentration profiles and the corresponding local equilibrium limit results.

The Effect of Altering Relative Rate Constants

The effect on the solution to the mass transport equations of changing the relative rate constants is considered with a simple example

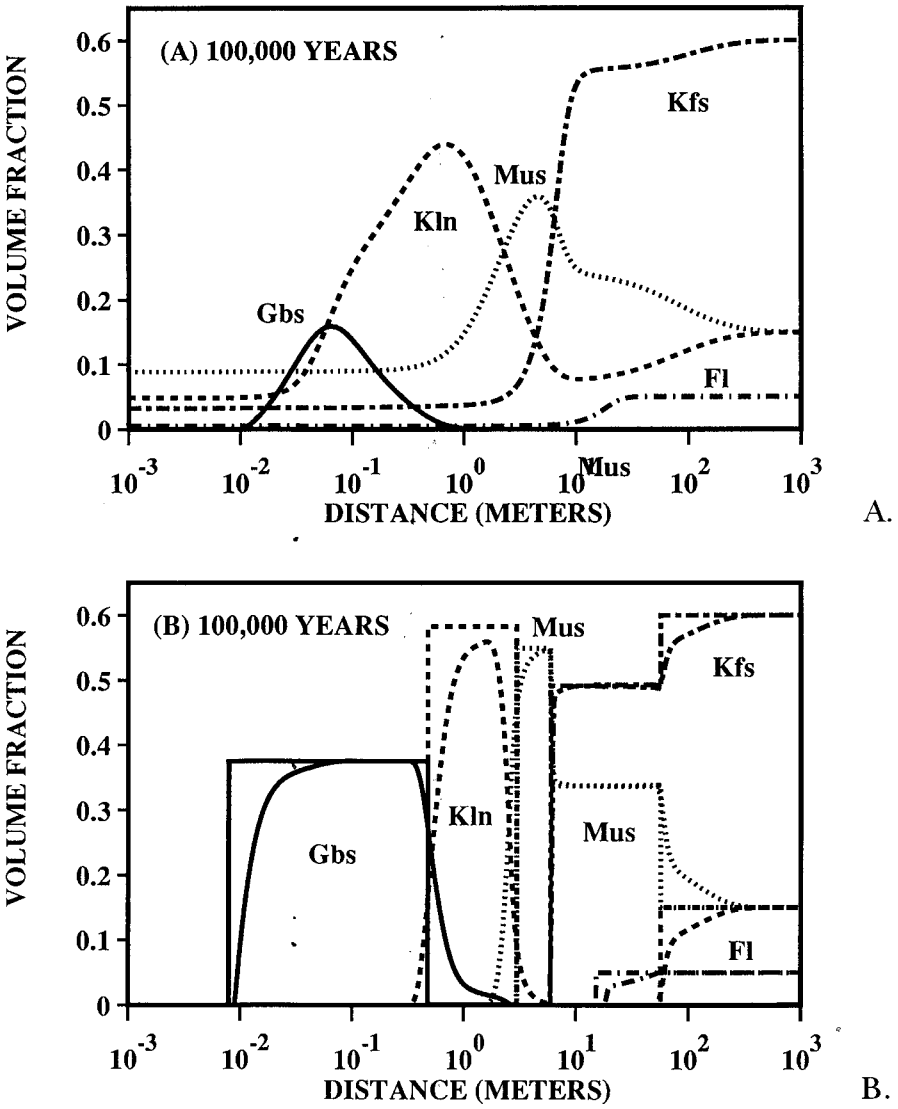

Fig. 7(A) Mineral modal abundances corresponding to the weathering of a hydrothermally altered phonolite host rock plotted as a function of depth after elapsed time of 100,000 yrs with the same conditions as in figure 6. (B) Mineral modal abundances are compared with the local equilibrium result given in table 1 for pure advective transport and the kinetic calculation corresponding to 2 my scaled by a factor of $\sigma = 20$.

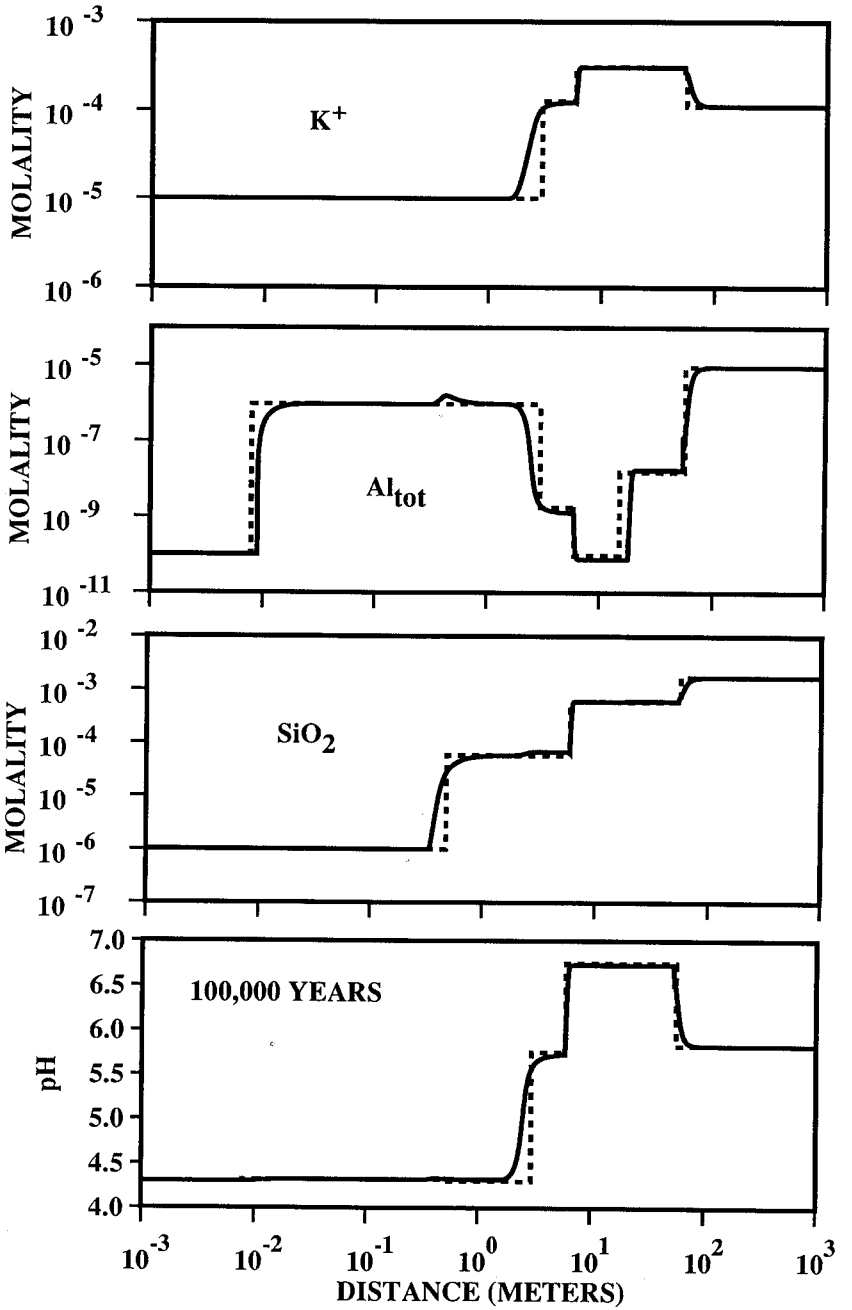

Fig. 8. Comparison between local equilibrium (dashed lines) and kinetic (solid curves) calculations for concentration of solute species K^+, Al_{tot}, SiO_2, and pH plotted as a function of distance after an elapsed time of 100,000 yrs for the same conditions as in figure 6. The kinetic results correspond to the solution at 2 my scaled by a factor of 20.

involving the weathering of K-feldspar. A fluid with an inlet pH of 4 percolates through a porous column consisting of 20 percent K-feldspar and 70 percent quartz by volume. This problem has been considered previously by Lichtner (1988). The normal reaction sequence obtained for conditions of local equilibrium is Gbs|Kln|⟨Mus⟩|Kfs, where the muscovite zone forms a ghost zone with zero width in the limit of pure advective transport (Lichtner and Balashov, 1992). This is also the sequence obtained in a kinetic calculation for effective rate constants of 10^{-14} moles cm^{-3} s^{-1} for gibbsite, kaolinite, and muscovite and 3×10^{-16} moles cm^{-3} s^{-1} for K-feldspar (Lichtner, 1988). An entirely different zone sequence can be obtained by drastically reducing the kinetic rate constant for kaolinite and including pyrophyllite as a possible secondary mineral. Effective rate constants of 2×10^{-16} and 10^{-14} moles cm^{-3} s^{-1} for kaolinite and pyrophyllite, respectively, are used in the calculation with the rate constants for the remaining minerals the same as above. In this case, because of the much slower rate of precipitation of kaolinite, silica and aluminum are not removed as rapidly from solution, and the fluid becomes supersaturated with pyrophyllite which precipitates as shown in figure 9. (It is of no consequence here that pyrophyllite normally forms only under high temperature conditions.) The zone sequence: Gbs|Kln|Pyr|Mus| Kfs, obtained in this case, apparently has no counterpart in local equilibrium. With increasing time it might be expected that the pyrophyllite zone would eventually disappear resulting in the normal local equilibrium sequence. This is because as the kaolinite zone continues to grow, eventually it becomes wide enough that, regardless of the rate of reaction of kaolinite, the fluid can nevertheless reach equilibrium with respect to kaolinite, and the pyrophyllite zone becomes unstable and dissolves. Suprisingly, however, this is not what happens as is shown in figure 10. In this figure the reaction front positions are shown as a function of time. With increasing time the pyrophyllite zone propagates with constant width and never disappears completely. Although this behavior is similar to that of a ghost zone, it is not know whether a local equilibrium solution exists with pyrophyllite stable. If such a solution did exist, it would imply that the local equilibrium limit is not unique. Further investigation is required to determine the nature of the pyrophyllite zone in the asymptotic limit.

DISCUSSION

Not all theoretical formulations of solute transport and mineral reaction can be scaled. There are several ways in which the transport equations may be altered to give solutions that do not satisfy scaling properties. One possibility is initial or boundary conditions that are not scale invariant. Flux boundary conditions, for example, are not scale invariant. Another example is a heterogeneous unaltered host rock containing an initial zonation pattern such as bedding planes. The widths of the reaction zones in the unaltered rock define a length scale for the system, and therefore the problem can not be scaled. In order for the

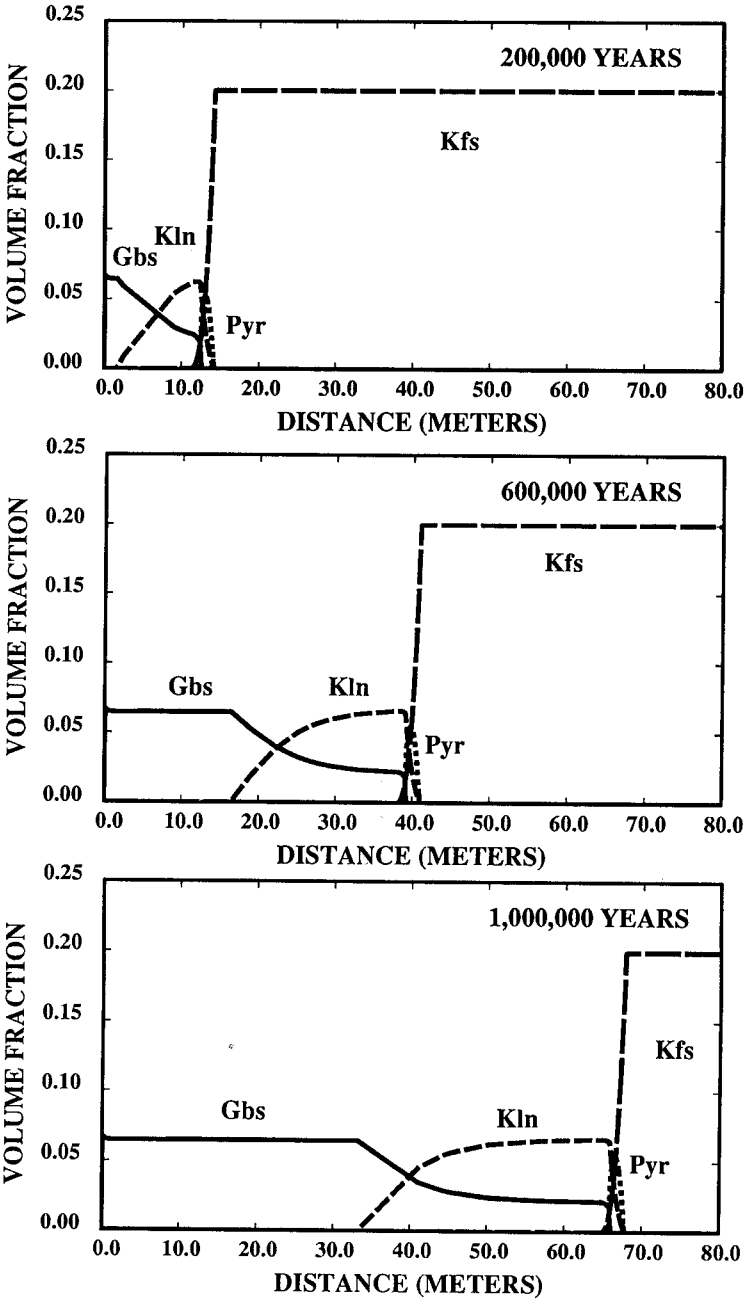

Fig. 9. Volume fractions plotted as a function of distance for the times indicated in the figure with a reduced rate constant for kaolinite of 10^{-16} mol cm^{-3} s^{-1}.

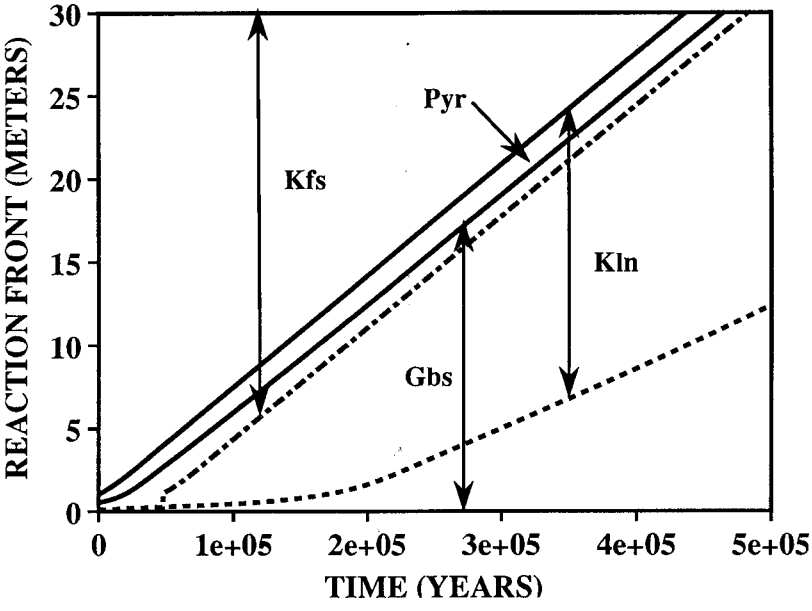

Fig. 10. Positions of the reaction zone boundaries plotted as a function of time for the same conditions as in figure 9.

transport equations to satisfy scaling properties, the initial composition host rock must be homogeneous and infinite in extent. Still another example of a problem that does not scale is the presence of a water table. It should be noted that the presence of a temperature gradient also leads to a problem that does not scale. Multiple porosity or more generally hierarchical porous media models probably do not satisfy scaling relations.

According to the general results presented here kinetic effects are important for relatively short time scales for which the system has not evolved for a sufficient amount of time to scale to the local equilibrium solution. Of course what constitutes enough time must depend on the type of host rock. Thus carbonate rocks would require a much shorter time compared to most silicate rocks, because of their faster reaction rates. A notable exception is nepheline syenite, for example, which also dissolves rapidly.

Advantages and disadvantages of a local equilibrium description.—In the case of pure advective transport the local equilibrium problem reduces to a set of algebraic equations for the solute concentrations, mineral volume fractions, and reaction front velocities (Walsh and others, 1984; Lichtner, 1991). Because of the inherent similarity between local equilibrium and kinetic descriptions, these equations provide an attractive alternative to the kinetic transport equations. They may be solved extremely rapidly compared to the kinetic transport equations, even for multicomponent

systems. However in many cases it is found that there does not exist a proper physical solution to these equations for the problem at hand (Lichtner, 1991). It has been found that it is necessary to introduce reaction zones of zero thickness, referred to as ghost zones, in order to obtain a consistent solution (Lichtner and Balashov, 1992). In this case, however, information is lost regarding, for example, the modal abundances of the ghost zone minerals. Alternatively, transport by diffusion must be included to obtain a complete description.

There are other cases, as well, where it appears that the limiting solution cannot be obtained from the algebraic equations representing the pure advective local equilibrium solution. These cases occur, for example, if a phase is allowed to become super-saturated in the kinetic problem without precipitating. Such circumstances do not seem possible to incorporate in the algebraic formulation of the local equilibrium problem.

Another major disadvantage of a local equilibrium description is that it is not possible to determine the correct sequence of reaction zones directly from the governing equations, contrary to a kinetic description for which the transport equations provide a unique determination of the reaction zone sequence. Finally for very short time spans the local equilibrium approximation cannot give an accurate description. In such cases a kinetic formulation of the problem is essential.

Estimating kinetic rate constants from the field.—Recent attempts to deduce kinetic rate constants from field observations of weathering profiles have resulted in values several orders of magnitude too low when compared with laboratory determined values (Pačes, 1983; Velbel, 1985). These estimates have assumed that the dissolution rate of a particular mineral in question is constant along the entire flow path and equal to its far from equilibrium rate. This assumption may not be justified, however, for sufficiently long flow paths and long time spans. In such cases the affinity factor occurring in the expression for the kinetic reaction rate must play a dominant role in determining the behavior of the solution. The effect of the affinity factor is to reduce the dissolution rate compared to the far from equilibrium value, becoming zero for a mineral in equilibrium with the fluid. As a consequence, reaction need only take place over a limited portion of the flow path to produce the change in solute concentration observed between two points along the flow path. The failure to appreciate the effect of the affinity factor on the reaction rate could therefore lead to a much smaller rate constant than otherwise would be necessary to explain the observed change in solute concentration.

According to the results of this study, because the velocities of the reaction fronts are determined by local equilibrium considerations and are independent of kinetics, if the overall rate of weathering is defined as the growth of the various reaction zones produced during weathering, then the weathering rate defined in this manner would be independent of kinetics. It must be emphasized, however, that sufficent time must have elapsed for distinct reaction zones to be produced in the first place

before these considerations can apply. For short time spans kinetics may be very important in determining the behavior of the system.

CONCLUSION

The scaling properties of time-space kinetic mass transport equations have significant implications on their solutions for problems in which the initial and boundary conditions are scale invariant. By scaling the time and space coordinates of the kinetic solution, it is possible to extract the local equilibrium limiting solution. Because scaling preserves the amplitudes of the solution concentration and mineral volume faction profiles, the kinetic and local equilibrium solutions are closely related. With increasing time the sensitivity of the kinetic solution on the expression for the reaction rate becomes less and less important in governing the behavior of the solution. A further consequence of the scaling properties is that solutions to the kinetic transport equations belonging to identical initial and boundary conditions, but corresponding to different rate constants, all tend toward the same limiting solution when scaled in time and space. This limiting form of the solution depends only on the thermodynamic properties of the system and not on the relative kinetic rate constants or reacting surface area. In some cases the limiting solution may be obtained directly by solving a set of algebraic equations representing the local equilibrium transport problem. In this sense the precise form of the rate expression is not as important to the final form of the solution as thermodynamic data. This would seen to be an important result, since if the solution were highly sensitive to the rate expression it would be an almost impossible task to describe natural systems because of their extreme complexity. Finally it was suggested that the reported discrepancy between field and laboratory derived kinetic rate constants may be, in part, a consequence of neglect of the affinity factor appearing in the expression for the kinetic rate law when attempting to determine the field based rate constant.

ACKNOWLEDGMENTS

Special thanks are due to Victor Balashov for an extensive review of the manuscript and for valuable discussions during the course of the work.

APPENDIX A

Scale transformation of the non-reactive transport equation

For a function f(x, t) defined as the solution to a differential equation, the consequences of scaling the independent variable can be deduced directly from the differential equation itself. As an example consider the solution to the non-reactive advection-diffusion equation. The solute concentration C(x, t; D, v) of a non-reactive species satisfies the partial differential equation

$$\frac{\partial C}{\partial t} + v\frac{\partial C}{\partial x} - D\frac{\partial^2 C}{\partial x^2} = 0, \tag{A.1}$$

where D designates the diffusion coefficient, and v represents the average fluid velocity. This equation has the well-known solution

$$C(x, t; D, v) = C_\infty + \frac{1}{2}(C_0 - C_\infty)\left\{\operatorname{erfc}\left[\frac{x - vt}{2\sqrt{Dt}}\right] + e^{vx/D}\operatorname{erfc}\left[\frac{x + vt}{2\sqrt{Dt}}\right]\right\}, \tag{A.2}$$

corresponding to the initial and boundary conditions

$$C(x, 0; D, v) = C_\infty, \qquad (0 \le x \le \infty), \tag{A.3}$$

and

$$C(0, t; D, v) = C_0, \qquad (0 \le t \le \infty), \tag{A.4}$$

where erfc(x) denotes the complementary error function.

Applying the scale transformation of the time and space coordinates given by eqs (4) and (5) leads to the transformed partial differential equation

$$\frac{\partial C}{\partial t_\sigma} + v\frac{\partial C}{\partial x_\sigma} - \sigma^{-1}D\frac{\partial^2 C}{\partial x_\sigma^2} = 0. \tag{A.5}$$

In addition the initial and boundary conditions are invariant with respect to the scale transformation. Because this equation has the identical form as the original equation if D is replaced by σ^{-1} D and is subject to the identical initial boundary conditions, the solution C(x, t; D, v) scales according to the expression

$$C(\sigma x, \sigma t; D, v) = C(x, t; \sigma^{-1}D, v). \tag{A.6}$$

as is easily verified. This result may also be obtained directly from the explicit form of the solution given in eq (A.2). The physical basis for the existence of the scaling relation is the lack of any inherent length or time scale in the problem. The result holds only if the initial and boundary conditions are invariant under the scale transformation. For example, if a flux boundary condition at the inlet were used, the scaling relation would no longer apply.

This relation may be used to deduce the effect of diffusion on the concentration profile. If a solution is known for one particular value of the diffusion coefficient D, it can be obtained for any other value D′ (including zero) merely by scaling the time and space coordinates of the original solution according to the relation

$$C(x, t; D', v) = C(\sigma x, \sigma t; D, v), \tag{A.7}$$

with

$$D' = \sigma^{-1}D. \tag{A.8}$$

The limit $\sigma \to \infty$ is of special interest, corresponding to D′ = 0, or pure advective transport. It follows that

$$\begin{aligned}\lim_{\sigma\to\infty} C(\sigma x, \sigma t; D, v) &= \lim_{\sigma\to\infty} C(x, t; \sigma^{-1}D, v)\\ &= \lim_{D\to 0} C(x, t; D, v)\\ &= C_0\,[1 - \theta(x - vt)] + C_\infty\theta(x - vt),\end{aligned} \tag{A.9}$$

where θ(x) denotes the Heaviside function defined by

$$\theta(x) = \begin{cases} 1 & (x < 0) \\ 1/2 & (x = 0). \\ 0 & (x < 0) \end{cases} \tag{A.10}$$

Accordingly, the pure advective limiting solution is obtained by scaling the time and space coordinates of the solution corresponding to combined advection and diffusion. As the diffusion coefficient tends toward zero, the solute concentration approaches a step-function with a jump discontinuity at the salinity front. The effect of diffusion on the solute profile, therefore, is to smear out the sharp change in concentration associated with the salinity wave by altering the time and length scales of the system.

Appendix B: *Local Equilibrium*

The local equilibrium approximation is defined as the limit in which the kinetic rate constants tend to infinity. In this limit the affinity tends toward zero, and the expression for the kinetic reaction rate approaches the indeterminate value $0 \cdot \infty$. The kinetic rate laws are replaced by algebraic constraints corresponding to mass action equations representing mineral equilibria. The transport equations describing mineral reactions in local equilibrium with an aqueous solution can be expressed in the form (Lichtner, 1985):

$$\frac{\partial}{\partial t}\left(\tilde{\phi}\tilde{\Psi}_j + \sum_m \nu_{jm}\overline{V}_m^{-1}\tilde{\phi}_m\right) + \frac{\partial \tilde{\Omega}_j}{\partial x} = 0, \tag{B.1}$$

where in what follows a tilde designates the local equilibrium limit. These equations are subject to the constraint equations

$$K_m \prod_{j=1}^{N} (\tilde{\gamma}_j \tilde{C}_j)^{\nu_{jm}} = 1, \tag{B.2}$$

representing equilibrium of the mth mineral. The reaction rates of minerals in local equilibrium with the aqueous solution may be calculated from the mineral transport equations

$$\tilde{I}_m = \overline{V}_m^{-1}\frac{\partial \tilde{\phi}_m}{\partial t}, \tag{B.3}$$

or, equivalently, from the solute transport equations

$$\tilde{I}_m = -\sum_\alpha (\nu^{-1})_{m\alpha}\left\{\frac{\partial}{\partial t}(\tilde{\phi}\tilde{\Psi}_\alpha) + \frac{\partial \tilde{\Omega}_\alpha}{\partial x}\right\}, \tag{B.4}$$

where $(\nu^{-1})_{m\alpha}$ denotes the inverse matrix to the stoichiometric reaction matrix ν_{jm}, and the subscript α runs over a set of primitive primary species (Lichtner, 1991). If the local equilibrium transport equations are interpreted as applying separately to each reaction zone, then additional equations are necessary specifying conservation of mass across each reaction front (Lichtner, 1985). These equations, referred to as the Rankine-Hugoniot relations, are given by

$$\tilde{v}_m^{(i)} = \frac{[\tilde{\Omega}_j]_i}{[\tilde{\phi}\tilde{\Psi}_j]_i + \Sigma_m \nu_{jm}\overline{V}_m^{-1}[\tilde{\phi}_m]_i}. \tag{B.5}$$

Integrating the Rankine-Hugoniot equations yields the positions of the reaction zone boundaries, denoted by $\tilde{l}_m^{(i)}(t; D, u)$, as functions of time.

Under a scale transformation of the time and space coordinates of the local equilibrium transport equations, with the flux Ω_j transforming according to eq (35), it follows immediately that the generalized concentration and mineral volume fraction transform according

to the equations

$$\tilde{\Psi}_j(x_\sigma, t_\sigma; \sigma^{-1}D, u) = \tilde{\Psi}_j(x, t; D, u), \tag{B.6}$$

and

$$\tilde{\phi}_m(x_\sigma, t_\sigma; \sigma^{-1}D, u) = \tilde{\phi}_m(x, t; D, u), \tag{B.7}$$

analogously to the kinetic field variables. Alternatively these relations can be expressed according to

$$\tilde{F}_\alpha(x, t; \sigma^{-1}D, u) = \tilde{F}_\alpha(\sigma x, \sigma t; D, u), \tag{B.8}$$

By introducing the field variable $\tilde{F}_\alpha$ to represent the solute concentration and mineral volume fraction. From this relation it follows that the solution corresponding to pure advective transport can be obtained from that incorporating diffusion by scaling the time and space coordinates. Thus taking the limit $\sigma \to \infty$, the left hand side approaches the pure advective limit, similarly to the non-reactive case. For pure advective transport in an isothermal porous medium the transport equations representing local equilibrium reduce to a set of algebraic equations (Walsh and others, 1984; Lichtner, 1991).

The scaling properties of the reaction zone boundaries in the case of local equilibrium follow directly from the Rankine-Hugoniot relations. Thus the reaction front velocities transform according to the relation

$$\tilde{v}_m^{(i)}(t_\sigma;\sigma^{-1}D, u) = \tilde{v}_m^{(i)}(t; D, u), \tag{B.9}$$

or, equivalently

$$\tilde{v}_m^{(i)}(t; \sigma^{-1}D, u) = \tilde{v}_m^{(i)}(\sigma t; D, u), \tag{B.10}$$

in agreement with the kinetic result, as follows from eq (B.5) making use of the scaling relations for Ψ_j and ϕ_m. From the definition

$$\frac{d\tilde{l}_m^{(i)}}{dt} = \tilde{v}_m^{(i)}, \tag{B.11}$$

the scaling properites of the positions of the zone boundaries can be determined with the result

$$\sigma\tilde{l}_m^{(i)}(t_\sigma; \sigma^{-1}D, u) = \tilde{l}_m^{(i)}(t; D, u), \tag{B.12}$$

or, equivalently

$$\sigma\tilde{l}_m^{(i)}(t; \sigma^{-1}D, u) = \tilde{l}_m^{(i)}(\sigma t; D, u). \tag{B.13}$$

From these relations it follows that with increasing time the velocities of the zone boundaries in the case with diffusion present approach the velocities corresponding to pure advective transport.

Single Component System

The remainder of this appendix considers the single component system discussed in section titled The Effects of Altering Relative Rate Constants. For the general case of combined advection and diffusion the solute concentration in the solute concentration in the local equilibrium limit is given by Lichtner (1988):

$$\tilde{C}(x, t; D, u) = \tilde{C}_-(x, t; D, u)(1 - \theta(x - \tilde{l}(t)) + C_{eq}\theta(x - \tilde{l}(t)), \tag{B.14}$$

with

$$\tilde{C}_-(x, t, D, u) = C_0 e^{x/\lambda} + [C_{eq} - C_0 e^{l/\lambda}] \frac{1 - e^{x/\lambda}}{1 - e^{l/\lambda}}, \tag{B.15}$$

and the mineral volume fraction is given by the relation

$$\tilde{\phi}_s(x, t; D, u) = \phi_s^\infty \theta(x - \tilde{l}(t)). \tag{B.16}$$

The position of the dissolution front is defined implicitly by the equation

$$\tilde{l}(t; D, u) + \lambda\left(\exp\left\{-\frac{\tilde{l}(t; D, u)}{\lambda}\right\} - 1\right) = \frac{vt}{K_\Delta}, \tag{B.17}$$

where K_Δ is defined in eq (C.13). The local equilibrium solution satisfies the scaling relations

$$\tilde{C}(\sigma x, \sigma t; D, u) = \tilde{C}(x, t; \sigma^{-1} D, u), \tag{B.18}$$

and

$$\tilde{\phi}_s(\sigma x, \sigma t; D, u) = \tilde{\phi}_s(x, t; \sigma^{-1} D, u), \tag{B.19}$$

similar to the non-reactive transport equations. The reaction front position scales according to the relation

$$\tilde{l}(\sigma t; D, u) = \sigma \tilde{l}(t; \sigma^{-1} D, u). \tag{B.20}$$

For conditions of pure advective transport the solute concentration is given by

$$\tilde{C}(x, t; u) = C_0(1 - \theta(x - \tilde{l}(t; u)) + C_{eq}\theta(x - \tilde{l}(t; u)), \tag{B.21}$$

representing a chemical shock front. The mineral volume fraction is given by eq (B.16). The position of the reaction front is given by

$$\tilde{l}(t; u) = \frac{vt}{k_\Delta}. \tag{B.22}$$

Appendix C

Single Component System

According to Lichtner (1988) the stationary state solute concentration can be expressed in the form

$$\begin{aligned} C(x, t; k, D, u) = {} & C_+(x, t; k, D, u)\theta(x - l(t; k, D, u)) \\ & + C_-(x, t; k, D, u)[1 - \theta(x - l(t; k, D, u))], \end{aligned} \tag{C.1}$$

and the mineral volume fraction is given by the expression

$$\phi_s(x, t; k, D, u) = \phi_s^\infty (1 - e^{-q(x - l(t;k,D,u))})\theta(x - l(t; k, D, u)). \tag{C.2}$$

The functions $C_\pm$ refer to the concentration on the upstream and downstream sides of the front $l(t; k, D, u)$, defined, respectively, by

$$C_+(x, t; k, D, u) = C_l + (C_{eq} - C_l)(1 - e^{-q(x - l(t;k,D,u))}), \tag{C.3}$$

and

$$C_-(x, t; k, D, u) = C_0 e^{x/\lambda} + [C_l - C_0 e^{l/\lambda}] \frac{1 - e^{x/\lambda}}{1 - e^{l/\lambda}}. \tag{C.4}$$

The inverse length q is defined by the equation

$$q(k, D, u) = \begin{cases} ks/u & (D = 0, \quad u \neq 0) \\ \sqrt{ks/\phi D} & (D \neq 0, \quad u = 0), \\ u(W - 1)/2\phi D & (D \neq 0, \quad u \neq 0) \end{cases} \tag{C.5}$$

for pure advection, pure diffusion and combined advection and diffusion, where

$$W(k, D, u) = \left[1 + \frac{4ks\phi D}{u^2}\right]^{1/2}. \tag{C.6}$$

The quantity λ denotes the characteristic diffusion length defined by

$$\lambda = \frac{D}{v}, \tag{C.7}$$

where v denotes the fluid velocity

$$v = \frac{u}{\phi}. \tag{C.8}$$

The solute concentration is continuous across the dissolution front with the value C_l at the front given by

$$C_l(t; k, D, u) = \frac{(C_{eq} + C_0/q\lambda)e^{l/\lambda} - C_{eq}}{(1 + 1/q\lambda)e^{l/\lambda} - 1}. \tag{C.9}$$

The equation of motion satisfied by the dissolution front l(t; k, D, u) can be determined by substituting eq (C.2) into eq (72) to give

$$v_l = \frac{dl}{dt} = \frac{1}{q\tau_0} \frac{C_{eq} - C_l}{C_{eq} - C_0}, \tag{C.10}$$

where τ_0 denotes the time for the solid to dissolve completely at the inlet, given by

$$\tau_0 = \frac{\phi_s^\infty \overline{V}_s^{-1}}{ks(C_{eq} - C_0)}. \tag{C.11}$$

As noted by Lichtner (1988) the front velocity can be rewritten in the form

$$v_l = \left[\frac{1}{\chi(l; k)}\right] \frac{v}{K_\Delta}, \tag{C.12}$$

where the quantity K_Δ is identical to the local equilibrium distribution coefficient for pure advective transport defined by

$$K_\Delta = \frac{\phi_s^\infty \overline{V}_s^{-1}}{\phi(C_{eq} - C_0)}, \tag{C.13}$$

and is independent of the kinetic rate constant. The function χ is defined by

$$\chi(l; k) = 1 - \frac{W(k, D, u) - 1}{W(k, D, u) + 1} e^{-vl/D}. \tag{C.14}$$

As the distance traveled by the front increases, χ tends exponentially to unity, and the front velocity approaches the local equilibrium velocity. For pure advective transport the front velocity is constant and identical to the local equilibrium result.

Explicit expressions for the positions of the reaction front l(t) may be obtained for pure advection, pure diffusion, and combined advection and diffusion by integrating eq (C.10) subject to the initial condition

$$l(\tau_0) = 0. \tag{C.15}$$

This gives the following results valid for $t \geq \tau_0$ for pure advective transport, pure diffusion and combined advection and diffusion (Lichtner, 1988). for pure advective transport the position of the solid dissolution front l(t; k, u) is given by

$$l(t; k, u) = \frac{1}{q\tau_0}(t - \tau_0). \tag{C.16}$$

For pure diffusion l(t; k, D) is given by

$$l(t; k, D) = \frac{2}{q\sqrt{2D\tau_0}}\sqrt{D(t - \tau_0}. \tag{C.17}$$

Finally for the case of combined advection and diffusion the dissolution front l(t; k, D, u) satisfies the transcendental equation

$$\left(\frac{1}{q\lambda} + 1\right)l(t; k, D, u) + \lambda\left(\exp\left\{-\frac{l(t; k, D, u)}{\lambda}\right\} - 1\right) = \frac{1}{\lambda q^2\tau_0}(t - \tau_0). \tag{C.18}$$

Scaling relations. The scaling relations for the solution concentration, mineral volume fraction, and reaction front position and velocity can be derived directly from the above equations making use of the following property of the Heaviside function

$$\theta(ax) = \theta(x), \tag{C.19}$$

for any constant a, and noting that

$$C_l(\sigma t; k, D, u) = C_l(t; \sigma k, \sigma^{-1}D, u), \tag{C.20}$$

$$q(\sigma k, \sigma^{-1}D, u) = \sigma q(k, D, u), \tag{C.21}$$

$$\tau_0(\sigma k) = \sigma^{-1}\tau_0(k), \tag{C.22}$$

and

$$W(\sigma k, \sigma^{-1}D, u) = W(k, D, u). \tag{C.23}$$

Under the scale transformation of the space and time coordinates given by eqs (4) and (5) that the solute concentration and mineral volume fraction satisfy the relations

$$C(\sigma x, \sigma t; k, D, u) = C(x, t; \sigma k, \sigma^{-1}D, u), \tag{C.24}$$

and

$$\phi_s(\sigma x, \sigma t; k, D, u) = \phi_s(x, t; \sigma k, \sigma^{-1}D, u), \tag{C.25}$$

in agreement with eq (39). The position of the dissolution front l(t) scales according to

$$l(\sigma t; k, D, u) = \sigma l(t; \sigma k, \sigma^{-1}D, u), \tag{C.26}$$

corresponding to eq (44). The velocity of the front satisfies the relation

$$v_l(\sigma t; k, D, u) = v_l(t; \sigma k, \sigma^{-1}D, u). \tag{C.27}$$

The local equilibrium limit is obtained from the scaling relations in the limit $\sigma \to \infty$. In this limit the concentration at the reaction front approaches the value

$$\lim_{\sigma\to\infty} C_l(\sigma t; k, D, u) = \frac{C_{eq} + C_0/q\lambda}{1 + 1/q\lambda} = \xi C_{eq} + (1 - \xi)C_0, \tag{C.28}$$

where

$$\xi = \frac{q\lambda}{1 + q\lambda}. \tag{C.29}$$

In the limit $\sigma \to \infty$, C and ϕ_s asymptotically approach the expressions

$$\lim_{\sigma\to\infty} C(\sigma x, \sigma t; k, D, u) = C_0[1 - \theta_\xi(x - \tilde{I}(t; u))] + C_{eq}\theta_\xi(x - \tilde{I}(t; u)), \tag{C.30}$$

and

$$\lim_{\sigma\to\infty} \phi_s(\sigma x, \sigma t; k, D, u) = \phi_s^\infty \theta(x - \tilde{I}(t; u)), \tag{C.31}$$

where $\tilde{I}(t; u)$ denotes the position of the reaction front for pure advective transport in the local equilibrium limit defined by eq (B.22) in app. B, and where θ_ξ denotes the modified Heaviside function defined by

$$\theta_\xi(x) = \begin{cases} 1 \ (x > 0) \\ \xi \ (x = 0) \\ 0 \ (x < 0) \end{cases}. \tag{C.32}$$

The limiting expression for the kinetic solute concentration as the scale factor tends to infinity differs only insignificantly from the local equilibrium limit given by eq (B.21) in appx B by the value of the concentration at the reaction front. In the limit $k \to \infty$, $\xi \to 1$ and the two expressions are identical.

References

Aagaard P., and Helgeson, H. C., 1982, Thermodynamic and kinetic constraints on reaction rates among minerals and aqueous solutions. I. Theoretical considerations: American Journal of Science, v. 282, p. 237–285.

Balashov, V. N., and Lebedeva, M. I., 1991, Macrokinetic model of the origin and development of a monomineralic bimetasomatic zone, *in* Perchuk, L. L., editor, Progress in Metamorphic and Magmatic Petrology. A memorial volume in honor of D. S. Korzhinskii: Cambridge, Cambridge University Press, p. 167–195.

Helgeson, H. C., Murphy, W. M., and Aagaard P., 1984, Thermodynamic and kinetic constraints on reaction rates among minerals and aqueous solutions. II. Rate constants, effective surface area, and the hydrolysis of feldspar: Geochimica et Cosmochimica Acta, v. 51, p. 3137–3153.

Lichtner, P. C., 1985, Continuum model for simultaneous chemical reactions and mass transport in hydrothermal systems: Geochimica et Cosmochimica Acta, v. 49, p. 779–800.

———— 1988, The quasi-stationary state approximation to coupled mass transport and fluid-rock interaction in a porous medium: Geochimica et Cosmochimica Acta, v. 52, p. 143–165.

———— 1991, The quasi-stationary state approximation to fluid/rock reaction: local equilibrium revisited, in Ganguly, J., editor, Diffusion, atomic ordering and mass transport: Advances in Physical Geochemistry, v. 8, p. 454–562.

———— 1992, Time-space continuum description of fluid/rock interaction: Water Resources Research, v. 28, p. 3135–3155.

Lichtner, P. C. and Balashov, V. N., 1992, Metasomatic zoning: appearance of ghost zones in limit of pure advective mass transport: Geochimica et Cosmochimica Acta, in press.

Lichtner, P. C., and Biino, G. G., 1992, A first principles approach to supergene enrichment of a porphyry copper protore. I. Cu-Fe-S-H_2O subsystem: Geochimica et Cosmochimica Acta, v. 56, p. 3987–4013.

Lichtner, P. C., and Waber, N., 1992, Redox front geochemistry and weathering: Theory with application to the Osamu Utsumi uranium mine, Poços de Caldas, Brazil: Journal of Geochemical Exploration, in press.

Murphy, W. M., Oelkers, E. H., and Lichtner, P. C., 1989, Surface reaction versus diffusion control of mineral dissolution and growth rates in geochemical processes: Chemical Geology, v. 78, p. 357–380.

Novak, C. F., Schechter, R. S., and Lake, L. W., 1989, Diffusion and solid dissolution/precipitation in permeable media: AIChE J., v. 35, p. 1057–1072.

Ortoleva, P., Auchmuth, G., Chadam, J., Hettmer, J., Merino, E., Moore, C. H., and Ripley, E., 1986, Redox front propagation and banding modalities: Physica, v. 19D, p. 334–354.

Pačes, T., 1983, Rate constants of dissolution derived from the measurements of mass balance in hydrological catchments: Geochimica et Cosmochimica Acta, v. 47, p. 1855–1863.

Schechter, R. S., Bryant, S. L., and Lake, L. W., 1987, Isotherm-free chromatography: propagation of precipitation/dissolution waves: Chemical Engineering Communications, v. 58, p. 353–376.

Steefel, C. I., and Van Cappellen, P., 1990, A new kinetic approach to modeling water-rock interaction. The role of nucleation, precursors, and Ostwald ripening: Geochimica et Cosmochimica Acta, v. 54, p. 2657–2677.

Velbel, M. A., 1985, Geochemical mass balances and weathering rates in forested watersheds of the southern blue ridge: American Journal of Science, v. 285, p. 904–430.

Waber, N., ms., 1990, Hydrothermal and supergene evolution of the Osamu Utsumi uranium deposit and the Morro do Ferro thorium-rare earth deposit (Minas Gerais, Brazil): Ph.D. thesis, University of Bern, 179 p.

Walsh, M. P., Bryant, S. L., Schechter, R. S., and Lake, L. W., 1984, Precipitation and dissolution of solids attending flow through porous media: American Institut of Chemical Engineering Journal, v. 30, p. 317–327.